N-BIT DIGITALLY TUNABLE ULTRA WIDE-BAND PULSE GENERATOR

by

SERTAÇ YILMAZ

Submitted to the Graduate School of Engineering and Natural Sciences
in partial fulfillment of
the requirements for the degree of
Master of Science

Sabancı University
Fall 2005

N-BIT DIGITALLY TUNABLE UWB PULSE GENERATOR

APPROVED BY:

Assist. Prof. Dr. İbrahim TEKİN …….

(Dissertation Supervisor)

Assist. Prof. Dr. Mehmet Keskinöz …….

Assist. Prof. Dr. Ayhan BOZKURT ……..…

Assoc. Prof. Dr Yaşar GÜRBÜZ ……..…

MSc. EE Cem KURAL …….

R&D Electronics & Control Tec. Manager, ARÇELİK A.Ş.

DATE OF APPROVAL: …….

to my dear parents for their support

ACKNOWLEDGEMENTS

I would like to thank my supervisor Assistant Professor İbrahim Tekin for his guidance and advice throughout my thesis. He helped me in every step of my thesis, read my numerous revisions and encouraged me to overcome the problems. I could not complete this difficult process without his advisement, enthusiasm and friendly support.

I also would like to thank my dissertation members, Ayhan Bozkurt, Mehmet Kekinöz, Yaşar Gürbüz, and Cem Kural, who offered guidance and support.

Not but not least I would like to thank my family for their endless love and patience. Their limitless tolerance made everything about me possible.

Lastly, I would like to thank my friends in Sabancı University for their support and enjoyment during the tedious laboratory hours.

N-BIT DIGITALLY TUNABLE ULTRA WIDE-BAND PULSE GENERATOR

ABSTRACT

In this thesis, a new digitally tunable UWB pulse generator for an impulse type of pulse generator is developed. The pulse generator is realized with a low cost simple circuitry by using Step Recovery Diode (SRD), PIN diodes and microstrip transmission lines which are employed in the many basic UWB pulse generation circuits. During the pulse generation process, the generator initially generates sharp edges by using a Step Recovery Diode (SRD) from an applied low frequency input sinusoidal signal, and then the sharp edges are converted into short pulses with desired durations by utilizing parallel short-circuited stub with variable lengths. These variable length stubs are acquired by PIN Diodes and microstrip transmission line sub-sections. By adjusting the lengths of the microstrip transmission line, variable duration UWB pulses can be obtained. Also by controlling stub with the N sub-sections digitally, 2^N variable duration UWB pulses can be obtained that is a significant improvement in UWB pulse generation. The digitally tunable UWB pulse generator has been designed, implemented during the studies by using microstrip line technology and yielded reasonable performance. Typical pulse durations varying from 550 to 1750 psec and from 900 to 2500 psec have been obtained experimentally for 2-bit and 4-bit pulse generator, respectively. Experimental results are also duplicated using simulations based on Agilent Advance Design System (ADS) platform.

SAYISAL OLARAK AYARLANABİLİR N KADEMELİ ULTRA GENİŞ-BANT İŞARET ÜRETECİ

ÖZET

Bu tezde, yeni bir sayısal olarak ayarlanabilir N kademeli ultra geniş-bant darbe tipi işaret üreteci geliştirilir. İşaret üreteci; birçok temel UWB işaret üretim devresinde yer alan step recovery diyot, PIN diyot ve iletim hatları kullanılarak düşük maliyetli basit bir devre ile gerçekleştirilir. İşaret üretim sürecinde, üreteç öncelikle uygulanan düşük frekanslı giriş sinüs sinyalinden step recovery diyotunu kullanarak dik kenarlar yaratır; daha sonra üretilen dik kenarlar, ayarlanabilir uzunluktaki parçalardan oluşan paralel kısa devre koçanından yararlanılarak, arzu edilen zaman genişliğinde dar işaretlere dönüştürülür. Bu ayarlanabilir uzunluktaki parçalar PIN diyotlar ve iletim hattı alt-bölümlerinden elde edilir. Alt-bölümlerdeki, mikroşerit iletim hattının boylarını ayarlayarak değişik zaman genişliğine sahip UWB işaretleri oluşturulabilir. Aynı zamanda , N alt-bölümden oluşan bir paralel koçanı sayısal olarak kontrol ederek, UWB işaret üretiminde çok önemli bir gelişme olan 2^N farklı zaman genişliğine sahip UWB işareti elde edilebilir. Çalışmalar sırasında mikroşerit teknolojisi kullanılarak, sayısal olarak ayarlanabilir UWB işaret üreteci tasarlanmış ve gerçeklenmiştir ve yeterli performans sağlanmıştır. Deneysel olarak gerçeklenen 2-kademeli ve 4-kademeli işaret üreteçlerinden sırasıyla 550 pikosaniyeden 1750 pikosaniyeye ve 900 pikosaniyeden 2500 pikosaniyeye değişen zaman genişliklerine sahip işaretler sağlanmıştır. Deneysel sonuçlar Agilent Advance Design System (ADS) yazılımı kullanılarak simülasyonlar ile de doğrulanmışlardır.

TABLE OF CONTENTS

LIST OF FIGURES

LIST OF TABLES

LIST OF ABBREVIATIONS

ADS	Advance Design System
DSP	Digital Signal Processing
DSSS	Direct Sequence Spread Spectrum
FCC	Federal Communication Commission
GPR	Ground Penetrating Radar
IC	Integrated Circuit
IR	Impulse Radio
OFDM	Orthogonal Frequency-division Multiplexing
PPM	Pulse Position Modulation
RF	Radio Frequency
S_{11}	Reflection Coefficient
SNR	Signal to Noise Ratio
SRD	Step Recovery Diode
UWB	Ultra Wide-band
WPAN	Wireless Personal Area Network

1. INTRODUCTION

Recently, there have been many military applications of UWB technology including ground penetrating radar (GPR), wall penetrating radar, secure communications and precision positioning/tracking [1, 2]. There is also an interest in civil use of UWB technology such as in Wireless Personal Area Networks (WPAN) [3, 4]. This concentration has been the result of growing demand for much advanced data rates on the order of hundreds of megabits since upcoming wireless networks require very large transmission bandwidths to achieve these data rates. Currently, nearly all wireless data technologies such as Bluetooth, IEEE 802.11b have baseband signals up to tens of megabits, and the baseband signal is transmitted using an RF carrier, which is mainly a narrowband communication technique.

FCC recently allocated the frequency range from 3.1 to 10.6 GHz for UWB communications. UWB signal can be identified as the signal that has the bandwidth to center frequency ratio greater than 0.25 or bandwidth of 500 MHz or higher. Generating UWB signal is essential assignment for the UWB technology. There are mainly two alternative approaches of UWB systems from the point of view of generating the UWB signal. These are single band approach and multiband approach. The single-band technique supports the idea of impulse radio that is the original approach to UWB by using narrow pulses that occupy a large portion of the spectrum. The multiband approach divides the available UWB frequency spectrum into multiple smaller and non-overlapping bands to obey the FCC's definition of UWB signals. In the impulse radio (IR), a single band technique, ultra narrow pulses in picoseconds are generated and the generated time pulses may span of a few GHz bandwidth [5]. It is easy to be implemented and has low probability of detection. It is mostly preferred in the GPR and precision positioning/tracking system. Direct-sequence Ultra Wide-band (DS UWB) is also a single-band approach that uses narrow UWB pulses and time-domain signal

processing combined with DSSS techniques to transmit and receive information. DS UWB uses a combination of a single-carrier spread-spectrum design and wide coherent bandwidth that provides low-fading, optimal interference characteristics, inherent frequency diversity and precision ranging capabilities [6]. These attributes mean DS-UWB is well suited to be the physical layer for PANs in multipath environments, such as homes. The other system is the multi-banded approach so that multiple narrowband signals are generated independently and then merged to form the larger bandwidth of UWB signal [7, 8]. The multi-banded orthogonal frequency-division multiplexing (OFDM) approach is used in the commercial UWB systems [9].

In this thesis, we concentrate on UWB IR method and we aim to develop a new UWB pulse generator. Current research work on UWB impulse radio concentrates on the development of miniaturized, efficient UWB pulse generators. The most recent works focus on the generation of the low power UWB pulses [10, 11]. The pulse generation methods in these papers produce pulses that approximate Gaussian monocycles quite well with simple circuits, which are shown in the **Appendix A** with simulation and measurement results. These pulse generator circuits include 3 main sections; impulse generator circuit, impulse shaping circuit, monocycle pulse forming circuit. The output of the impulse generator circuit is a Gaussian-like pulse waveform so that the impulse shaping circuit is employed to convert it to Gaussian monocycle pulse which has band-pass frequency spectrum, which result in less demanding design specifications for other system components like antennas. Both the impulse generator circuit and the monocycle pulse forming circuit utilize almost the same procedure with little differences.

In the recent studies on UWB pulse generation, an electronically tunable pulse generator is developed which is capable of varying the pulse duration electronically for the GPR transmitter and receiver systems [12]. Therefore, the generator circuit produces N UWB pulses with different pulse widths by using N PIN diodes/transmission line sub-sections. In the impulse GPRs, the pulse widths of the generated time pulses have influence on the resolution of the radar. If the impulse radio is used as GPR to provide high penetration depth, higher pulse durations are preferred; however, it also brings about low resolution. Decreasing of the sounding pulse duration and increasing the resolution is considered as one of the most promising ways for increase the quality of primary GPR data. However, excessively high resolution can also have inverse effect. Rather, use of more durational sounding signals can improve the primary GPR data

[13]. Therefore, tuning the pulse width of the signal provides more flexibility and improved performance in UWB application systems. Particularly, in UWB ground penetrating radar, a tunable pulse generator allows the pulse width to be changed to achieve varying penetration depths and resolution. The pulse generator circuit explained in the thesis is handled with digitally in order that 2^N UWB pulses can be generated by employing only N PIN diode/transmission line sub-sections, which is a new achievement in the UWB IR systems.

This thesis includes the principles, technology and performance test results of such the new low-cost, compact ultra-wideband microstrip pulse generators capable of varying the pulse duration digitally. Representative pulse-duration variations from 550 to 1750 psec and from 900 to 2500 psec have been obtained experimentally for 2-bit and 4-bit pulse generator, respectively.

The organization of this thesis will be as follows:

In Chapter 2, the general principles and applications of the Ultra-wideband technology are investigated and the traditional UWB pulse waveforms are reviewed. The overall UWB transmitter and receiver system with pulse position modulation (PPM) and channel modeling is discussed throughout this chapter.

In Chapter 3, the basic principles of the suggested N-bit digitally tunable UWB pulse generator are presented. The process of the design and implementation of the pulse generator is explained theoretically and practically. Chapter 3 also introduces the some of difficulties of the proposed tunable pulse generation method like multiple reflections over the transmission lines. These reflections cause the output pulse of the system to be distorted. It also includes the modifications of the system to prevent the reflections.

In Chapter 4, the results of many simulations and experimental results, realized for measuring the performance of two different UWB pulse generators, are discussed. This chapter also includes limitations of the pulse generator circuits like specifications of the components and the implementation conditions. Lastly, conclusions and future work are given in Chapter 5.

2. THEORY OF ULTRA WIDEBAND TECHNOLOGY AND TRANSMITTER/RECEIVER SYSTEMS

UWB technology, being familiar with its use in GPR, has also been of significant concentration on communications and radar applications requiring low probability of intercept and detection (LPI/D), multipath protection, high data rates, precision ranging and localization. UWB technology is easily defined as any wireless transmission method that occupies a fractional bandwidth of more than 25% of a center frequency, or more than 500 MHz apart from fractional bandwidth and emissions below -41.3 dBm/MHz. UWB is just a mean of 7500 MHz of unlicensed spectrum. After a short introduction to the principles of ultra wideband technology, the advantages and the challenges of the UWB technology are explained and an overall UWB transmitter and receiver architecture is modeled as an example.

2.1 PRINCIPLES OF THE UWB TECHNOLOGY

UWB signals are usually defined as signals having an instantaneous bandwidth of 25% of the center frequency or no less than 500 MHz. To generate such signals, data symbols are carried by a set of very short pulses. A more general modulation scheme consists in transmitting spaced pulses trains. These time domain pulse waveform may include Gaussian mono-pulse (1^{st} and 2^{nd} derivative), Gaussian doublets, which combined two monocycles, Rayleigh monopulse and other complex shapes. The pulse bandwidth and spectrum are important since

- The pulse width defines the bandwidth
- Cycles per pulse defines center frequency

- Packet of the pulse spectrum defines the energy structure outside the main lobe in power spectrum

A figure of a uniformly spaced Gaussian monocycle (0.5 nsec pulse width) pulse train is shown in **Figure 2.1.1**.

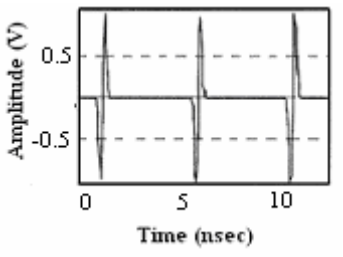

Figure 2.1.1 Gaussian Monocycle and associated power spectrum

By enveloping the spectrum with single band approach, Gaussian monocycle as shown in **Figure 2.1.2**, has the widest bandwidth, can work fine in multipath. However, it has the lowest flexibility in spectrum design and the shaping needs high performance silicon solutions. Few band approaches as shown in **Figure 2.1.3** can use cheaper IC technology in lower band and upper band later. On the contrary, it has moderate flexibility. Many band OFDM approach, shown in **Figure 2.1.4**, has excellent spectral flexibility, good multipath characteristics. But it needs DSP; thus it is generally used in the civil UWB systems.

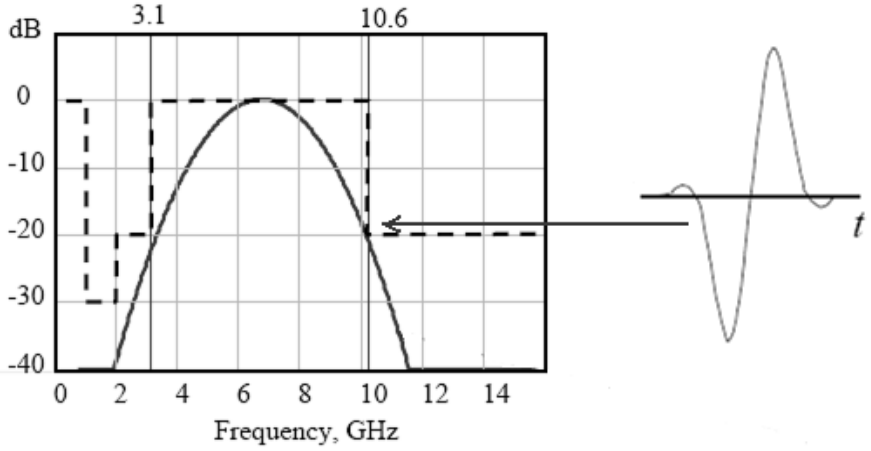

Figure 2.1.2 Single band approach

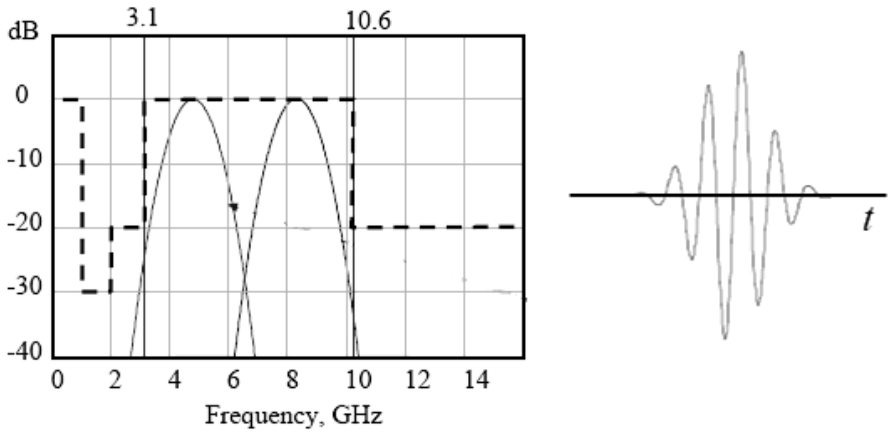

Figure 2.1.3 Few bands approach

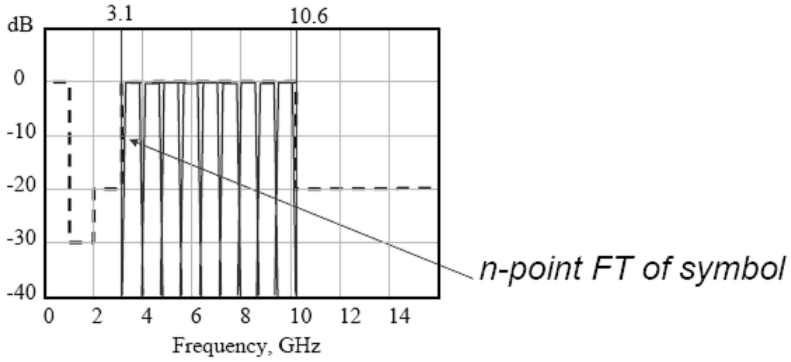

Figure 2.1.4 Many OFDM approach

In order to transmit information, it is obligatory to modulate the pulse train. One conventional modulation used in UWB is Pulse Position Modulation. In this technique, the temporal positions of the pulses are varied in accordance with the information data. For instance, a digital zero can be coded by transmitting the pulse about x psec earlier than a reference position and a digital one by transmitting the monocycle x psec later. More generally, many positions can be utilized to increase the amount of symbols. If there are n positions, the modulation is called n-PPM.

After having presented the properties of the UWB signal and its transmitting, the next topic is optimal receiving system. The first process to be carried out is matched filtering of the waveform in order to introduce a first level of demodulation. In order to do this, the incoming signal is multiplied with a reference waveform and the result is then integrated by integrate and dump circuit, as seen is **Figure 2.1.5**. This correlation

operation between the received signal and a local pattern (usually a local image of the received pulse waveform) has to be performed for each possible pulse position. Then, the correlation results are sent to the baseband for further processing. The correlation process and the correlator signal is also shown and discussed in next overall system simulation section.

As UWB emissions are generally low power, the received signal can be buried in the ambient noise. To overcome this problem, the receiver has to sum numerous correlator samples from subsequent pulses so that the noise, which has a zero average, will be considerably reduced. This process, called "coherent integration", allows the transmitted signals to be recovered.

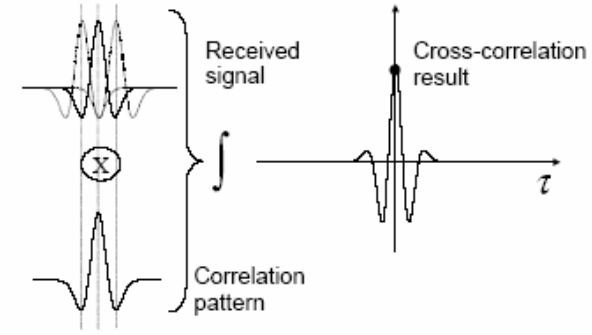

Figure 2.1.5 Correlation with reference

2.2 ADVANTAGES OF THE ULTRA WIDEBAND TECHNOLOGY

Commonly used modulation schemes for data transmissions by means of radio link (HiperLAN, 802.11) still rely on a traditional phase and/or amplitude modulated carrier based signal. For these techniques, the bandwidth is limited and the signal to noise ratio is quite good. If we want to increase the data rate, given the Shannon formula:

$$C = W \log_2(1 + SNR) \tag{2.1}$$

There are two possibilities that we can increase either the signal to noise ratio (SNR) or the bandwidth (W). The channel capacity increases linearly with the bandwidth and only logarithmically with the signal to noise ratio. For low power high

data rate applications, it is preferable to increase the bandwidth rather than the signal to noise ratio. The main idea of UWB is to transmit data symbols below the allowed unintentional emission level, -41.3 dBm/Hz, but on a bandwidth which extends over several gigahertz. This concept is based on the radiation of very short pulses and consequently the associated spectrum extends over a very wide frequency range as shown in **Figure 2.2.1**.

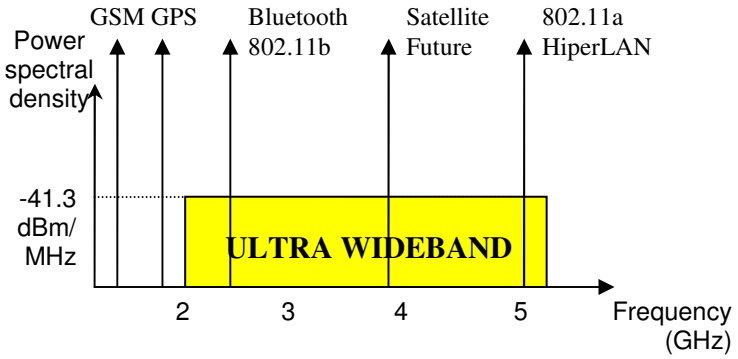

Figure 2.2.1 Comparison of UWB transmission with other communication protocols

Moreover, for communication concerns, the UWB concept has several advantages:

- Companies do not want to pay for new spectrum licenses. And there is no such large frequency available, anyway. This is why UWB transmissions concentrate on regarding the FCC spectrum mask, normally used to regulate unintentional radiation from consumer devices such as TVs, hair dryers, etc. In addition, this allows reusing allocated spectrum resources by suppressing the average signal under the noise floor.
- Short pulses suffer less from self-interference like fading and inter-pulse interference than continuous transmission of a modulated sine wave. This is why the UWB based system is an excellent contestant for high density of multipath channels such as indoor environments. The receiver can resolve all echoes and exploit the whole multipath energy spreading.
- Short pulses naturally extend energy among a large frequency range.
- The transmitted energy is fully contained in the data symbol with no carrier, which optimizes the power consumption and makes it a good candidate for mobile applications.
- The sequential discontinuity, which can be introduced between two consecutive pulses, allows an extra level of pulse position modulation.

• Low probability of detection and interception because of the spread of energy over a wide frequency range with a very low spectral power density.

• Low complexity, RF and analogue circuitry are reduced to a wideband low noise amplifier, a correlator and an integrator. There is no need for heterodyne architecture, which will result in a significant reduction of the transceiver area as well as the power. As compared with traditional radio transceiver architectures, the relative simplicity of UWB transceivers could yield important benefits.

An example of a low-cost, short-range wireless architecture is the Bluetooth radio, which is shown in **Figure 2.2.2** [4].

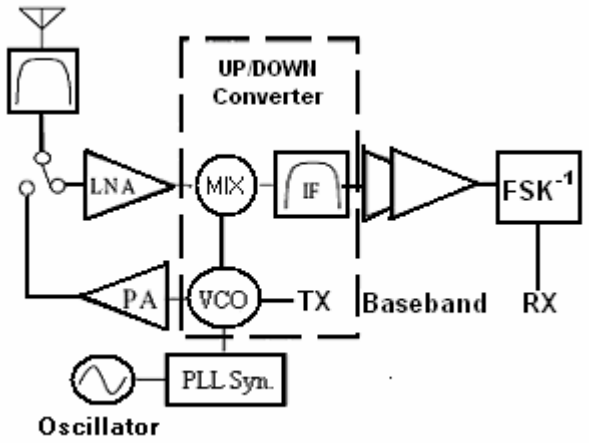

Figure 2.2.2 Example Bluetooth transceiver

Bluetooth uses a form of Frequency Shift Keying where information is sent by shifting the carrier frequency high or low. In the figure, this is achieved by applying the information bits, which is identified as TX in the figure to a Voltage-Controlled Oscillator (VCO). A Phase-Lock Loop synthesizer with a crystal reference oscillator is necessary to keep this oscillator's average frequency within spectrum. In receive mode, the extremely weak signal from the antenna is first amplified by low noise amplifier (LNA) and then down-converted to an Intermediate Frequency (IF). The down-converter uses a heterodyne technique where a non-linear mixer (MIX) is fed both the desired signal and a synthesized local oscillator that operates at a frequency either above or below the desired signal. The mixer produces an excess of images of the desired signal where each image is centered at the sum and difference terms of the desired signal and the local oscillator and harmonics. The image that falls at the desired IF

frequency passes through the IF filter, while the other images are rejected. At this low frequency, it is relatively easy to provide the stable high-gain circuits needed to demodulate the signal and recover the original information. Note that in higher performance radio systems, such as cellular phones, two or even three down conversion stages may be employed.

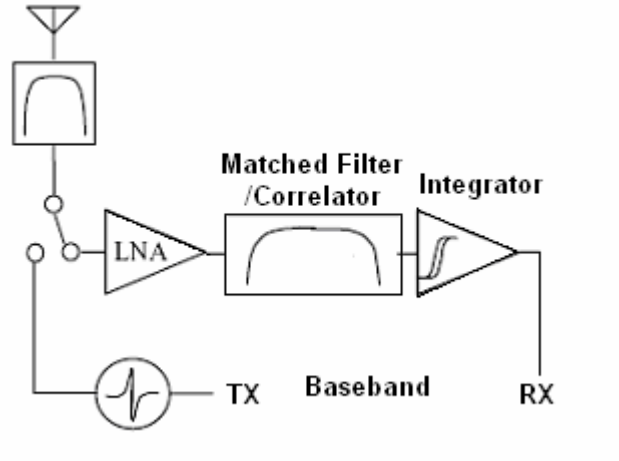

Figure 2.2.3 Example UWB transceiver architecture

A prototypical UWB transceiver is shown in **Figure 2.2.3**. This transceiver could be used for the same applications targeted for use with Bluetooth, but at higher data rates and lower emitted RF power. The pulse has a duration on the order of hundreds psec and its shape is designed to concentrate energy over the broad range of gigahertz. A power amplifier may not be required in this case because the pulse generator need only produce a low voltage swing on the order of hundred mV. A band pass filter is used before the antenna to restrict the emissions within the desired frequency band. In receive mode, the signal received by the antenna is amplified and passed through either a matched filter or a correlation-type receiver. A matched filter has an impulse response matched to the received pulse shape and will produce an impulse at its output when presented with RF energy which has the matching pulse shape. The original information is then recovered with an adjustable high-gain threshold circuit. Notice the relative simplicity of this implementation compared to the super-heterodyne architecture. This transceiver has no reference oscillator, Phase-Lock Loop (PLL) synthesizer, VCO, mixer, or power amplifier. This simplicity translates to lower material costs and lower assembly costs.

2.3 CHALLENGES OF THE UWB SYSTEM

Despite the advantages, there are still some design challenges for UWB RF transmitter and receiver. There is a concern that such a wide-band receiver will be liable to being unintentionally jammed by current narrowband transmitters that operate within the UWB receiver's passband. Also for such a wide-band impulse, designing a suitable antenna may be a complicated task, and there are issues that have to be resolved such as filter matching accuracy, which can often be difficult to achieve. For a correlator-based receiver, timing needs to be very accurate in order to properly detect the received pulse due to the short pulse duration. In addition to these challenges, Rake-type receiver may be used for improving performance since significant amount of energy in the multipath components in the channel part.

2.4 OVERALL ULTRA WIDEBAND TRANSMITTER AND RECEIVER SYSTEM MODELING

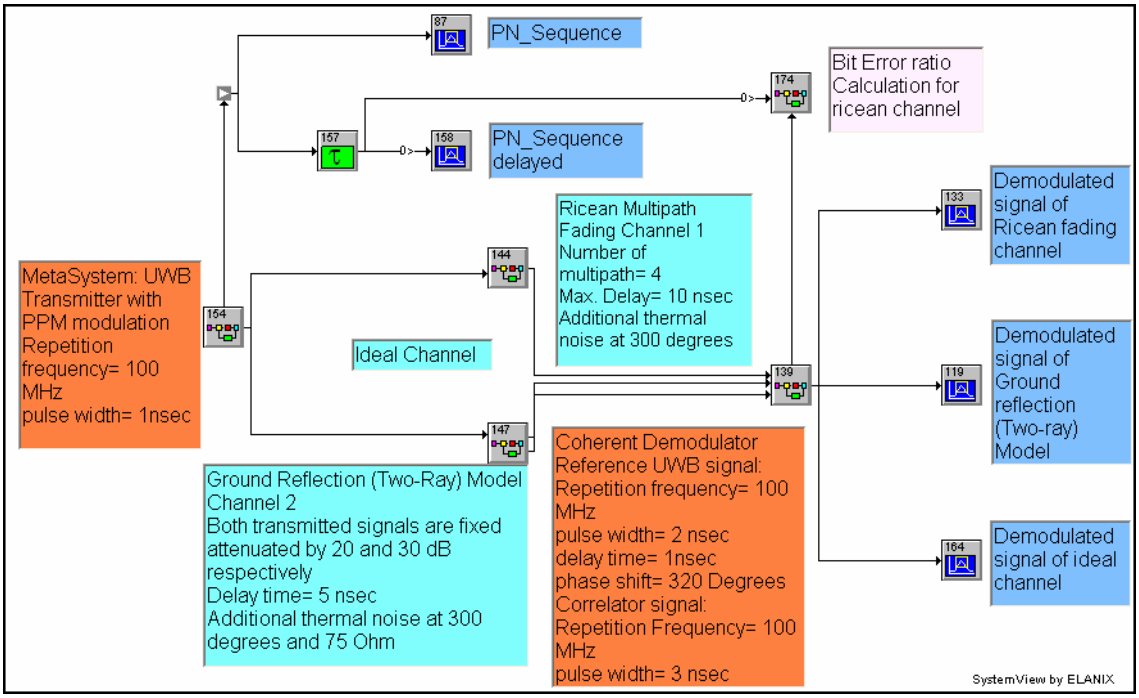

Figure 2.4.1 Ultra-Wideband System with MetaSystems containing pulse-shaping filters, transmitter, channels and the receiver

The overall UWB system is modeled and simulated by using the Elanix simulator of System View in order to demonstrate the simplicity of the UWB transceiver architecture, the function and the importance of the pulse generator in the system.

2.4.1 UWB Transmitter Using Pulse Position Modulation (PPM)

The UWB system, in **Figure 2.4.1,** uses pulse position modulation (PPM) in order to transmit information [14, 15]. The clock for the modulator is a 100 MHz square wave (10 nsec between rising edges). The output of the modulator is a very short pulse (2 nsec duration) that occurs some time after the rising edge of the 100 MHz clock. A detailed description of the PPM follows. At the modulator's front end as shown in **Figure 2.4.2**, the data to be transmitted is represented by a 2-level, bipolar (+/-1.0 volts), PN sequence, which is referred to as PN sequence, and may be seen in the plot in **Figure 2.4.3**. A 100.0 MHz clock driving an analog integrate-and-dump circuit creates a -1 volt 100 MHz ramp signal.

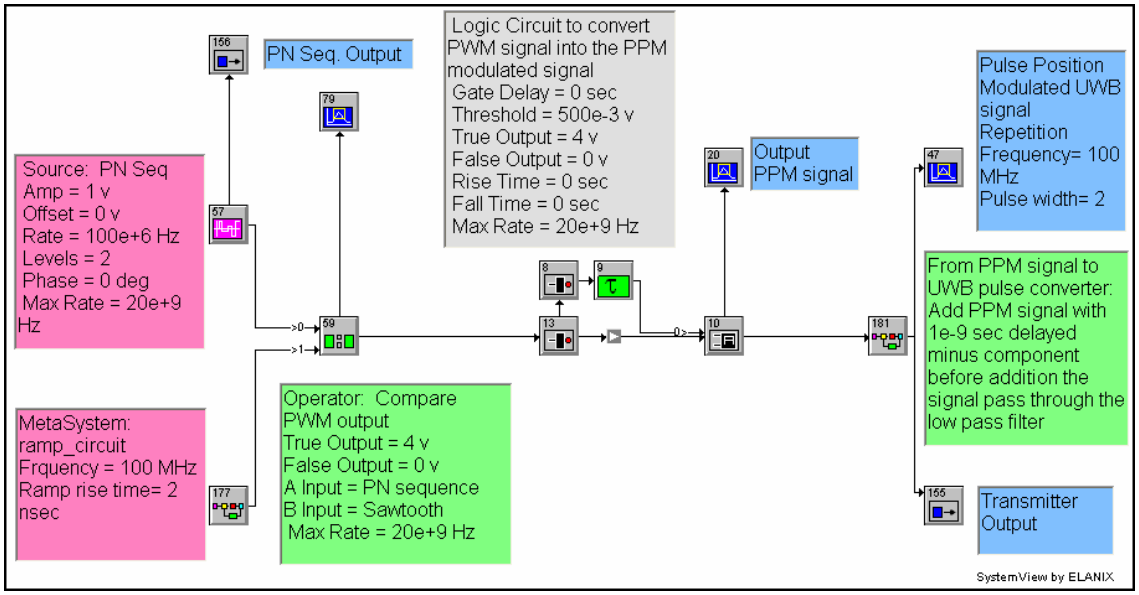

Figure 2.4.2 Ultra wideband transmitter with PPM

The comparator compares the PN sequence signal and the ramp and then the pulse width modulated (PWM) signal of the PN sequence is obtained as shown in

Figure 2.4.4. The output of the comparator contains the position information and goes to a digital differentiator circuit that is built from two NOT-gates, a delay, and an AND-gate. The digital differentiator circuit puts out a single thin (1 nsec) LOW-to-HIGH pulse for every LOW-to-HIGH transition output from the comparator. The AND-gate output amplitude parameters set the transmitter's output power.

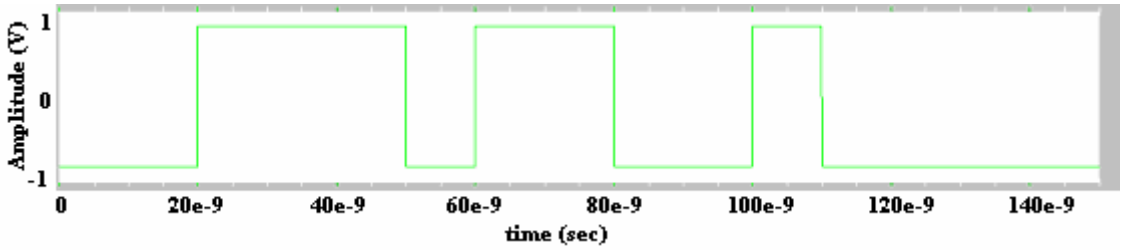

Figure 2.4.3 Input PN sequence

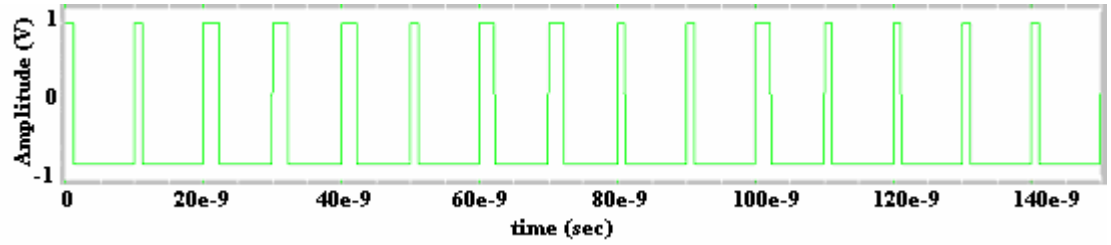

Figure 2.4.4 PWM signal at the output of the comparator

The unipolar, 0.0 to +4.0 volt pulses from the AND gate carry the information in the PPM which is given in **Figure 2.4.5**. For binary code 0, a 1 nsec length pulse is produced which is placed 1 nsec from the beginning of the period and for binary code 1, a 1 nsec length pulse is produced which is placed 2 nsec from the beginning of the period. Therefore, the information pulses are noise resistant because they are narrowband and they use only 3 nsec of the 10 nsec period. PPM signals are applied to a metasystem as shown in **Figure 2.4.6**, which is a filter block containing passive components. In the Metasystem, the pulse stream is split into two paths using a 2-way, 180-degree splitter. Each of the paths has a 4.0 GHz low pass filter; however the bottom path also has a 1e-9 sec delay. A positive-going pulse and a delayed, negative-going pulse added. In **Figure 2.4.7**, the upper and lower signal paths have been combined using a 2-way, 0-degree combiner. The combiner's loss is 3.5 dB.

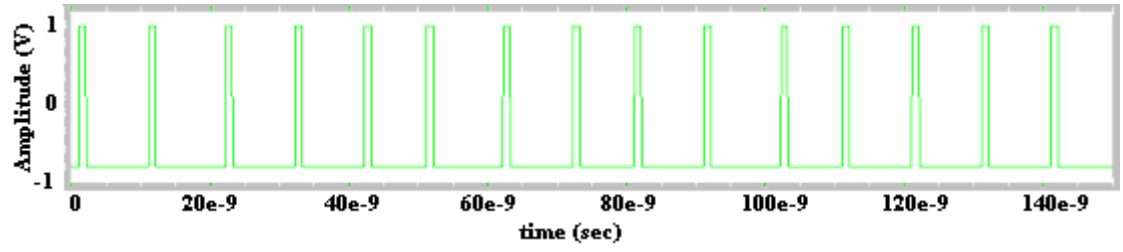

Figure 2.4.5 Output PPM signal of the digital differentiator

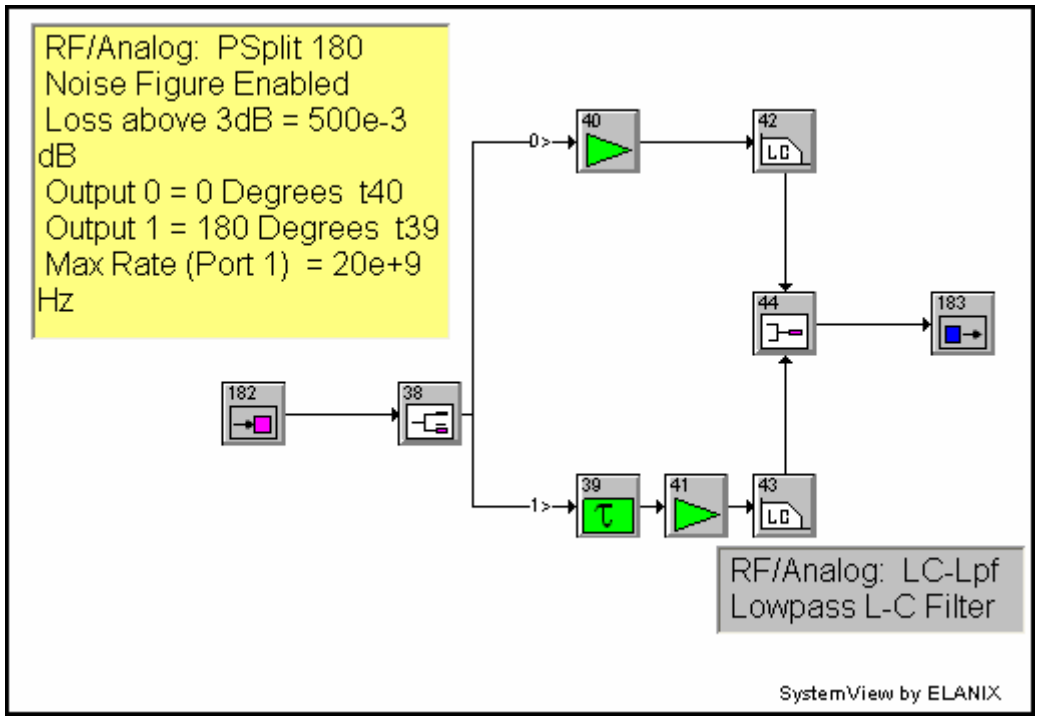

Figure 2.4.6 A view inside the MetaSystem containing the pulse-shaping circuit

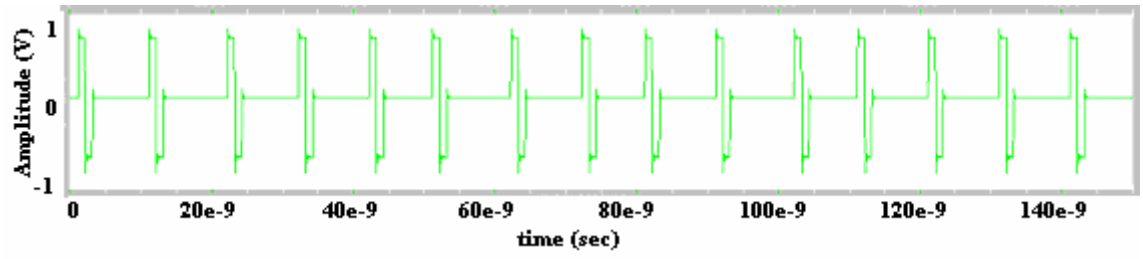

Figure 2.4.7 monocycle pulse at the output of the 0-degree combiner in previous figure

2.4.2 Channels, Path Loss and Antenna Noise

In **Figure 2.4.2**, the transmitter's output goes through 3 channels with different characteristics and antenna noise is added to the signal in the two of the channels before it enters the receiver Metasystem. One of the channels is an ideal channel, no attenuation and no delay, in order to control the overall system. The next one is Ricean Fading channel named as Channel 1. There are 4 multipaths and K-factor is adjusted to 0.5 with 10 nsec maximum delays. The signal after channel characteristics of channel 1 may be seen in the **Figure 2.4.8.** And the last one is Ground Reflection (Two-Ray) Model Channel that is named as Channel 2**.** In channel 2, both transmitted signals are attenuated by 20 and 30 dB respectively by the fixed attenuators, and then one of the attenuated signals is delayed with 5 nsec as the reflected from the ground. These signals are combined before adding noise to the channel. The channel response may be seen in the **Figure 2.4.9**. Also, thermal noise with 100 Ohm at 300 K degrees is combined with the channel 1 and channel 2. Then the signal goes to the receiver.

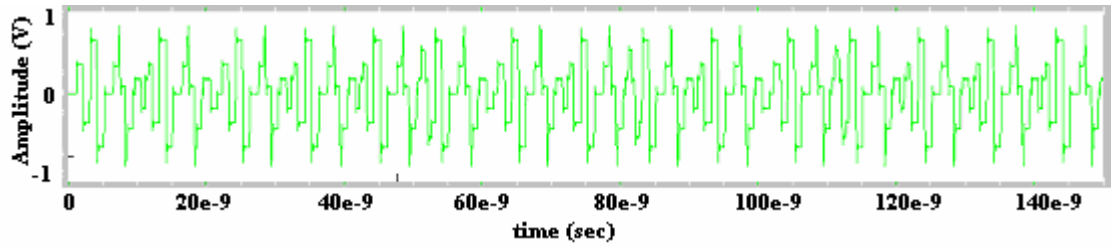

Figure 2.4.8 Signal after Ricean fading channel response

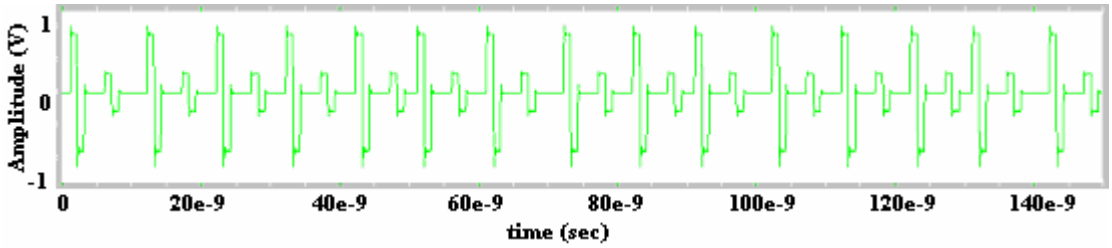

Figure 2.4.9 Two-Ray model Channel Response

2.4.3 UWB Receiver

The contents of the UWB pulse detector MetaSystem are shown in **Figure 2.4.10**. A coherent demodulator is used as the UWB receiver in this simulation. Therefore a correlator signal is designed for correlating with the channel outputs. In order to produce the correlator signal, first a reference UWB pulse train is formed which is shown in the **Figure 2.4.11**. Then the pulse train which works with 10 nsec period and 1 nsec pulsewidth with 320 degrees phase shift is applied to the UWB pulse converter. The converter is explained in the transmitter part. After getting reference UWB pulse train, it is combined with a negative UWB pulse train, which works at same frequency and is shifted by 1 nsec. The process can be seen in the figure of the coherent detector. The combination of two Gaussian Monocycles (First derivative of Gaussian wave) in the explained method gives us Gaussian Doublet (Second derivative of Gaussian wave) so that our correlator signal is similar to doublet, which is shown in the **Figure 2.4.12**. The correlator signal is multiplied with channels' outputs, and then the results are integrated and dumped with continuous 10 nsec integration time as a part of coherent demodulator. The last thing in the receiver to recover the input data is threshold device. We compare the output of the integrate and dump circuit with 0 volt and demodulated signal is get for ideal channel, Ricean Fading channel and Two-Ray Model channel which may be seen in the **Figure 2.4.13**, **Figure 2.4.14** and **Figure 2.4.15**. Their figures are good agreement with the input signal in **Figure 2.4.3.**

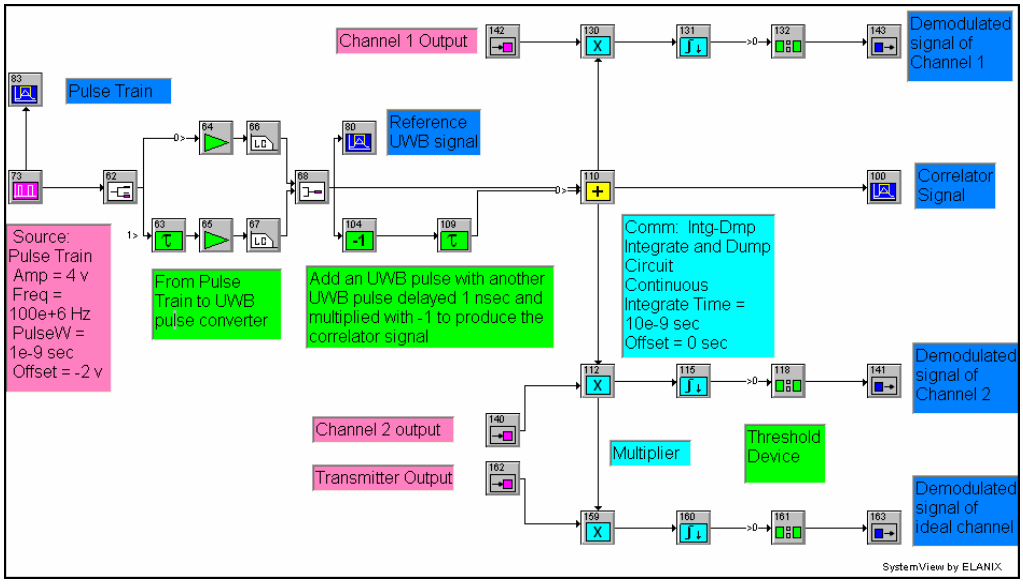

Figure 2.4.10 Ultra wideband Coherent Detector

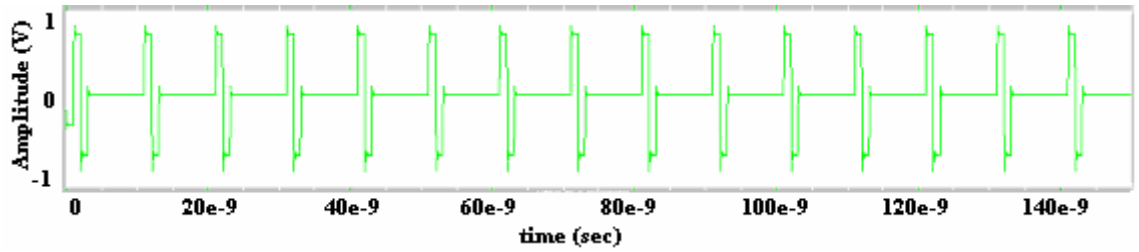

Figure 2.4.11 Reference UWB pulse

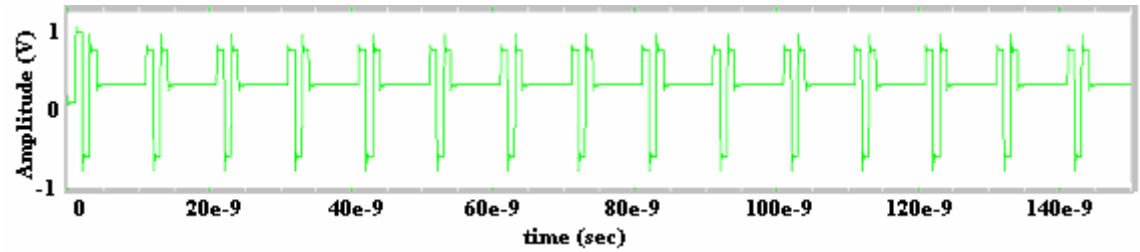

Figure 2.4.12 Correlator signal

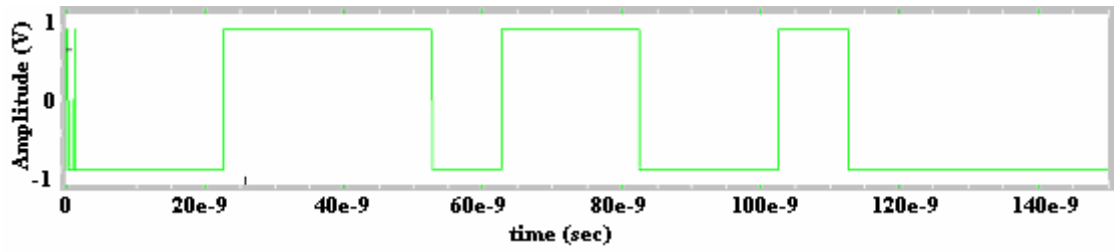

Figure 2.4.13 Demodulated signal of ideal channel

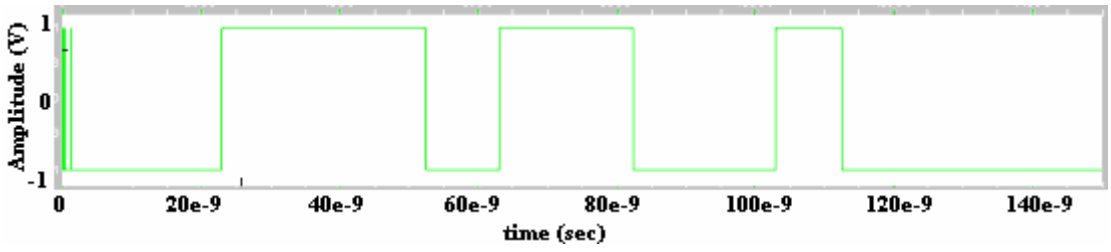

Figure 2.4.14 Demodulated signal of Ricean Fading Channel

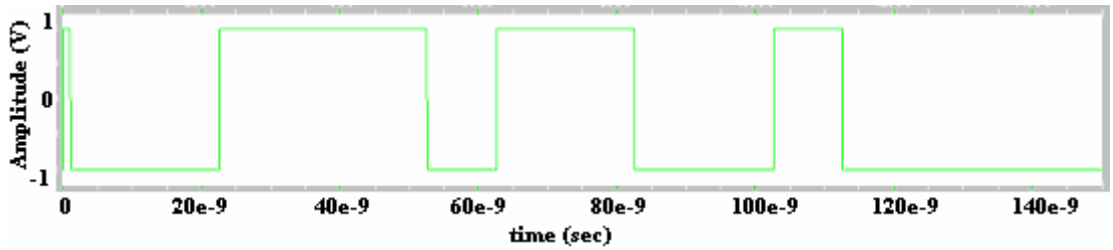

Figure 2.4.15 Demodulated signal of Two-Ray Model

3. N-BIT DIGITALLY TUNABLE UWB PULSE GENERATOR

In this chapter, the principles of the proposed digitally tunable UWB pulse generator circuit are presented. As mentioned before, at Chapter 2, the UWB pulse generators generate the UWB pulses with either fixed or electronically variable pulse width duration by utilizing two methods: using a Step Recovery Diode (SRD) impulse shaping circuit and then a parallel connected short circuit stub with a fixed delay line, or using a SRD impulse shaping circuit and then a parallel connected short circuit stub with electronically controllable and series connected PIN diodes/transmission line sub-sections which have different lengths. In this thesis, N series connected alternative PIN diode switches with transmission lines are used to obtain 2^N different durations.

3.1 AN OVERVIEW OF THE UWB PULSE GENERATION PRINCIPLE

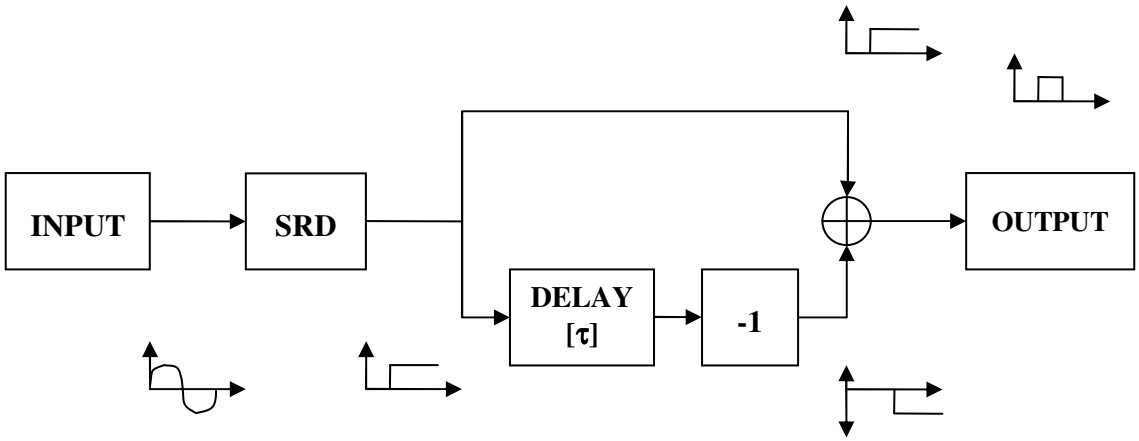

Figure 3.1.1 Flow graph of basic pulse generation

The flow graph of the pulse formation is basically shown in the **Figure 3.1.1**. The basic formation of an UWB pulse is obtained first by creating a sharp edge by using SRD, then the sharp edge being splitted into two components which are followed through two different signal paths and last combining them. One signal component goes directly to the circuit output, the other component is delayed by the phase shifter circuit and also the polarity of the pulse is reversed through the use of a short circuit. The summation of these two components will yield the desired UWB pulse at the output. In the **Figure 3.1.2**, generation of the pulse is mathematically modeled. **Figure 3.1.2(a)** shows the generated sharp edge with 1 Volt amplitude and 200 psec rise time by SRD, which will be explained later in detailed. In **Figure 3.1.2(b)**, the 400 psec delayed version of the sharp edge with the opposite polarity is shown and the sum of the figures generates the desired pulse as shown in **Figure 3.1.2(c)**. Note that, the same circuitry can be used to obtain a Gaussian Monocycle waveform, in other words; adding two mono pulses back to back with one of them being with opposite polarity generates a Gaussian monocycle waveform.

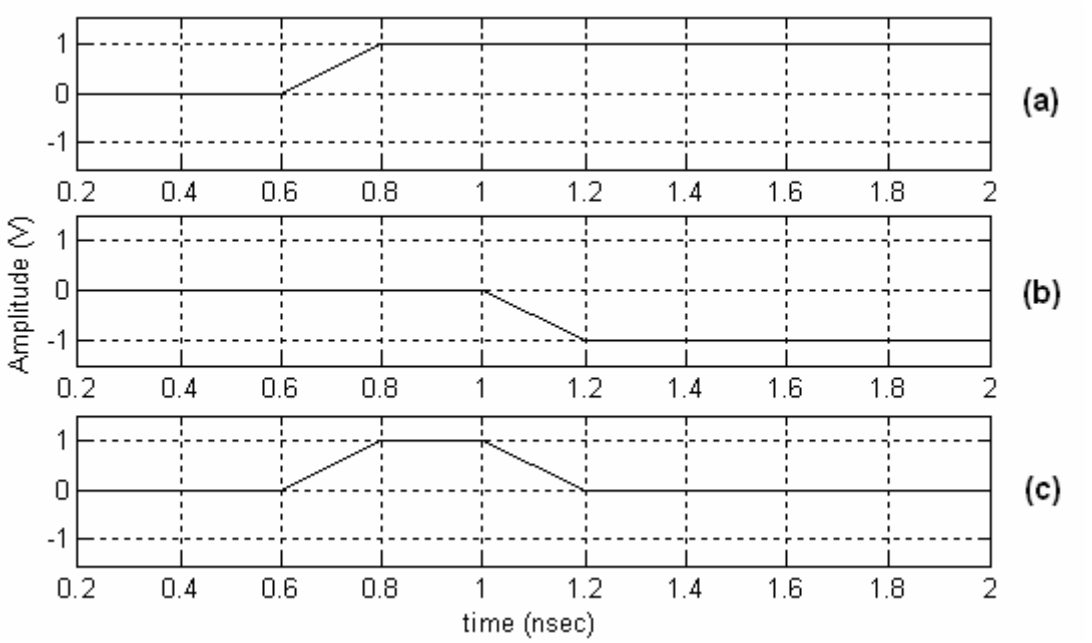

Figure 3.1.2 (a) A sharp edge obtained by using the SRD **(b)** the delayed version of the sharp edge with the opposite polarity **(c)** Sum of (a) and (b) to generate the desired pulse

3.2 WORKING PRINCIPLE OF THE CIRCUIT

N-bit digitally tunable UWB pulse generator is implemented with two main sub-circuits; Step Recovery Diode (SRD) impulse shaping circuit and the Phase Shifter circuit as shown in **Figure 3.2.1**. The figure shows the input step recovery diode (SRD) impulse shaping circuit, phase shifter circuit with N PIN diodes/transmission line sub-sections and the output load.

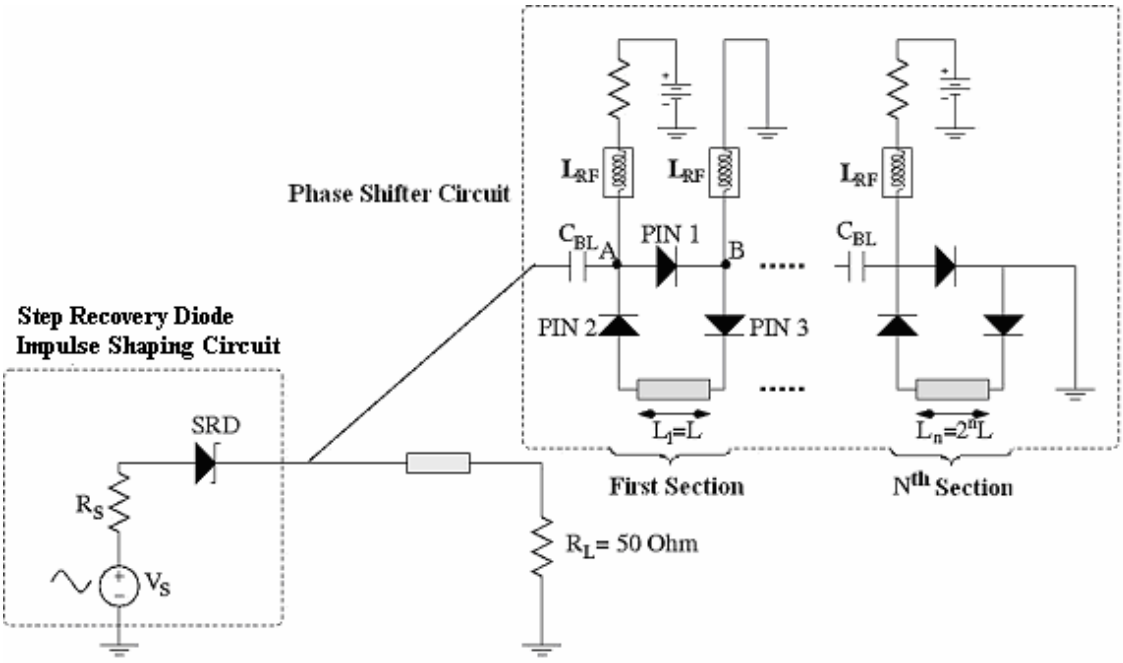

Figure 3.2.1 Schematic of the N-Bit digitally tunable pulse generator

3.3 STEP RECOVERY DIODE (SRD) IMPULSE SHAPING CIRCUIT

3.3.1 Definition of SRD

Step recovery diodes (SRDs) have remained extremely useful in wave-shaping applications in the last few decades since they were first presented. No other device rivals their combination of fast switching speed and ease of use [16]. **Figure 3.3.1** shows the two typical circuit configurations for SRD pulse sharpening. In both circuits, the SRD is initially biased with a constant forward bias current I_{DC}, which stores charge

in the SRD. When the voltage source V_{IN} rises, reverse biasing the SRD, the SRD conducts for a short period of time, removing the stored charge. This keeps the voltage across the diode very low. Then the stored charge is abruptly exhausted, and the SRD switches to a high-impedance, high-voltage state, resulting in a sharpening of the output voltage waveform. Therefore in the step recovery diode circuit, the SRD generates a sharp edge on the order of picoseconds from a low frequency sinusoidal signal applied to the input port of SRD diode circuit.

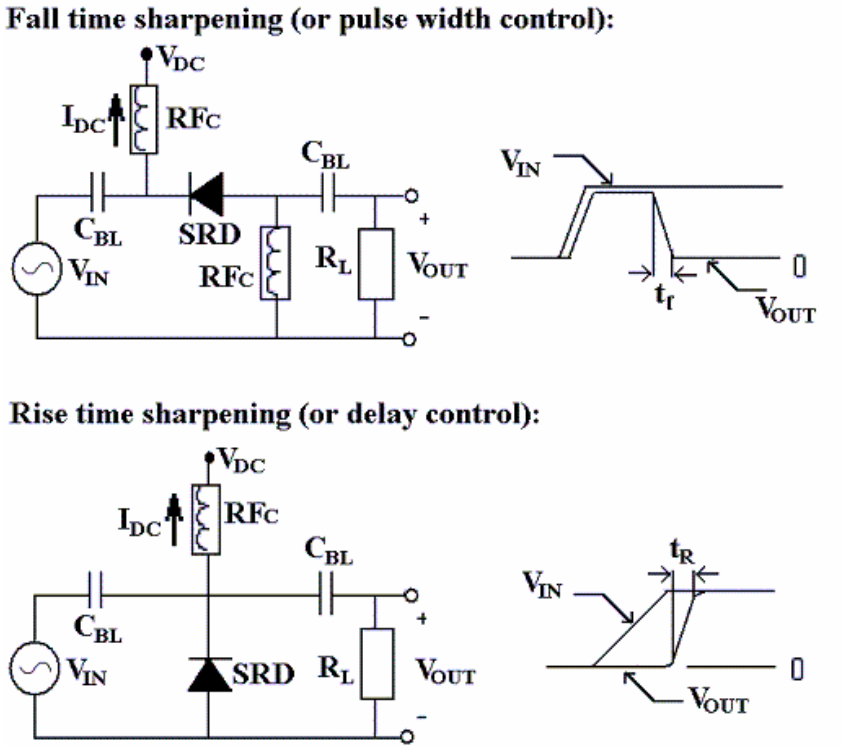

Figure 3.3.1 Standard step recovery diode pulse sharpening circuits

3.3.2 Biased SRD impulse shaping circuit

In Agilent ADS platform, both biased and unbiased versions of the SRD impulse shaping circuits were simulated. In **Figure 3.3.2**, the biased SRD pulse shaping circuit is shown in which input sinusoidal signal is at 10 MHz with 4 Volts amplitude, the diode is biased with -6 Volts amplitude DC supply and modeled according to records in the datasheet of SRDs of the Micrometrics Inc. The circuit is also implemented and tested on the FR4 glass epoxy high frequency substrate.

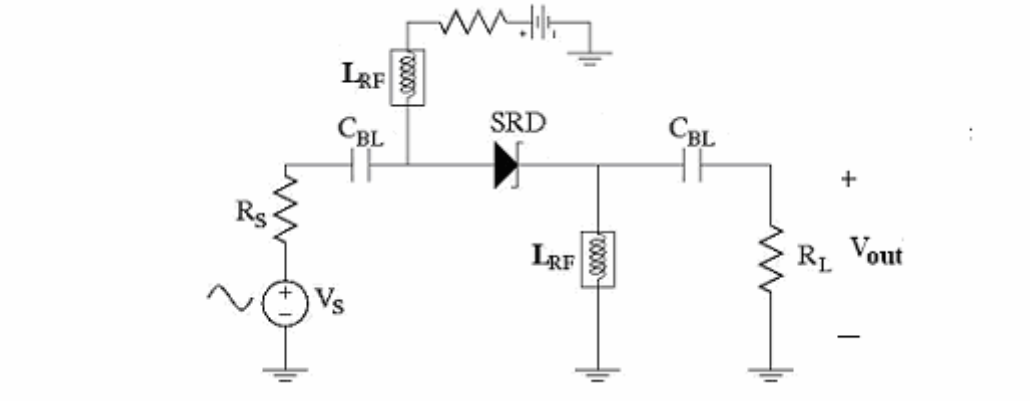

Figure 3.3.2 The schematic of the biased SRD pulse shaping circuit

In the simulation results of the SRD circuit given in **Figure 3.3.3**, the positive fall time of the input sinusoidal signal is sharpened with short transition time. The sharp edges are necessary for the generation of the pulse and the generated sharp edges are repeated with the period of the input signal. In the next chapter, the importance of transition time of the SRD is notified in detailed.

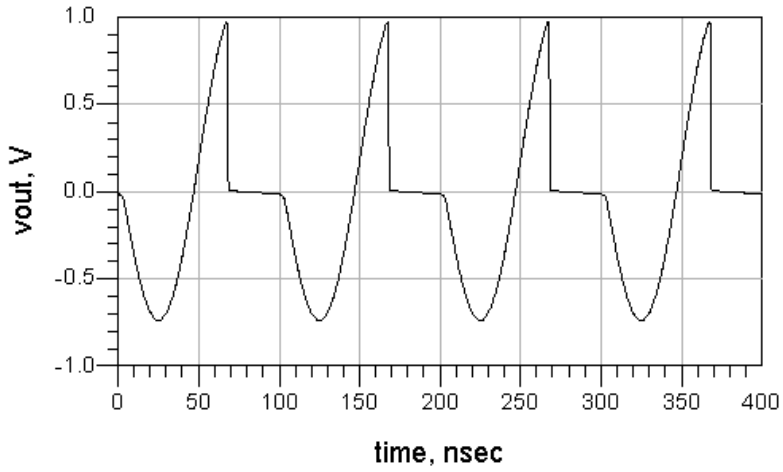

Figure 3.3.3 Simulation result of the biased SRD pulse shaping circuit

3.3.3 Unbiased SRD impulse shaping circuit

The fall time of the input signal can be also sharpened by the unbiased SRD impulse shaping circuit. The unbiased SRD circuit shown in the **Figure 3.3.4** is simple

to construct because no DC supply, DC blocking capacitors and RF chokes are employed in the circuit and the system is still sharpening the fall time of the input signal as well as the biased version. However, the amplitude of the output signal is limited since the current flow over the SRD is limited in the unbiased circuit with the amplitude of the input signal.

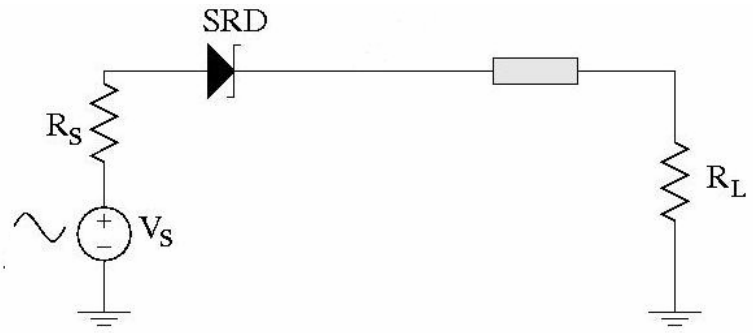

Figure 3.3.4 The schematic of the unbiased SRD pulse shaping circuit

Therefore, the impedance matching and the bias voltage are so important in the SRD impulse shaping circuit. The sharp edges cannot be generated unless the impedance matching of the input and the output is satisfied. Also, the bias voltage is so important that voltage swing cannot be obtained without biasing the circuit. In our thesis, a low power UWB pulse generator was chosen to be designed so that the unbiased SRD pulse shaping circuit could be sufficient for the UWB pulse generation and make the system easy to be realized.

3.4 PHASE SHIFTER CIRCUIT AND PIN DIODES/TRANSMISSION LINE SUB-SECTIONS

3.4.1 Theory of the Circuit

The phase shifter circuit is connected in parallel to the SRD circuit, and the main purpose of the phase shifter circuit is to delay the sharp edge generated by the SRD, and to reverse the polarity of the delayed edge by a short circuit, which terminates the phase shifter (or delay line) circuit. Actually, the phase shifter circuit is a true time delay

circuit. In addition to SRD circuitry, phase shifter circuit implemented with microstrip lines constitutes the rest of the UWB pulse circuit. The phase shifter circuit consists of N PIN diodes/transmission line subsections and every sub-section of a phase shifter circuit includes a microstrip transmission line, PIN diodes, RF chokes (L_{RF}), a DC blocking capacitor (C_{BL}) and a DC supply.

3.4.2 Microstrip Transmission Lines

Microstrip transmission lines are one the most popular types of planar transmission lines that are fabricated by photolithographic processes and easily integrated with passive and active microwave devices. The geometry of a microstrip line is shown in **Figure 3.4.1(a)**. A conductor of width W is printed on a thin, grounded dielectric substrate of thickness d and relative permittivity ε_r; a sketch of the field lines is shown in **Figure 3.4.1(b)**.

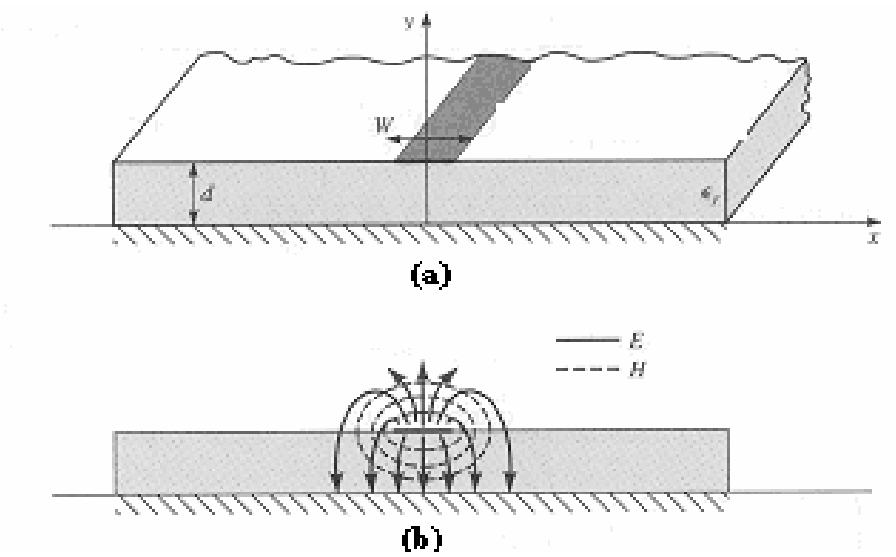

Figure 3.4.1 Microstrip transmission line **a)** Geometry **b)** Electric and magnetic field lines

The phase velocity, length and characteristic impedance of transmission lines can be obtained from static solutions. Then the phase velocity can be expressed as

$$v_p = \frac{c}{\sqrt{\varepsilon_e}} \tag{3.1}$$

where v_p is the phase velocity in m/sec, c is the velocity of light and ε_e is the effective dielectric constant of the microstrip line. Since some of the field lines are in the dielectric region and some in air, the effective dielectric constant satisfies the relation,

$$1 < \varepsilon_e < \varepsilon_r$$

and is dependent on the substrate thickness (d), and conductor width (W). The effective dielectric constant of a microstrip line is given approximately by

$$\varepsilon_e = \frac{\varepsilon_r + 1}{2} + \frac{\varepsilon_r - 1}{2} \frac{1}{\sqrt{1 + 12\frac{d}{W}}} \tag{3.2}$$

The effective dielectric constant can be interpreted as the dielectric constant of a homogeneous medium that replaces the air and dielectric region of the microstrip. Equation (3.3) relates the length of the transmission line to the desired delay and phase velocity that it is given by

$$l = \Delta t \times v_p \tag{3.3}$$

where l is the length in meters and Δt is the desired time delay in seconds. Given the dimensions of the microstrip line, the characteristic impedance can be calculated as

$$Z_0 = \begin{cases} \frac{60}{\sqrt{\varepsilon_e}} \ln\left(\frac{8d}{W} + \frac{W}{4d}\right) & \text{for } \frac{W}{d} \le 1 \\ \frac{120\pi}{\sqrt{\varepsilon_e}\left[\frac{W}{d} + 1.393 + 0.667 \ln\left(\frac{W}{d}\right) + 1.444\right]} & \text{for } \frac{W}{d} \ge 1 \end{cases} \tag{3.4}$$

for a given characteristic impedance Z_0 and dielectric constant ε_r, the *W/d* ratio can be found as

$$\frac{W}{d} = \begin{cases} \dfrac{8e^A}{e^{2A}-2} & \text{for } \dfrac{W}{d} < 2 \\ \dfrac{2}{\pi}\left[B-1-\ln(2B-1)+\dfrac{\varepsilon_r-1}{2\varepsilon_r}\left\{\ln(B-1)+0.39-\dfrac{0.61}{\varepsilon_r}\right\}\right] & \text{for } \dfrac{W}{d} > 2 \end{cases} \tag{3.5}$$

where

$$A = \frac{Z_0}{60}\sqrt{\frac{\varepsilon_r+1}{2}} + \frac{\varepsilon_r-1}{\varepsilon_r+1}\left(0.23+\frac{0.11}{\varepsilon_r}\right)$$

$$B = \frac{377\pi}{2Z_0\sqrt{\varepsilon_r}}$$

The transmission lines are used as the delay elements and the attenuators in the high frequency circuits. The circuit in **Figure 3.4.2** is simulated in ADS in order to demonstrate the transfer characteristic of the transmission lines. The characteristic impedance of the transmission line is adjusted to the load impedance, thus the width is calculated by using equations (3.2) and (3.5). As a result, the output signal becomes the delayed version of the input signal with little attenuation. The simulation result is shown in **Figure 3.4.3**. The amount of the delay between the input and the output signals is adjusted with the length of the transmission line calculated by equations (3.1), (3.2) and (3.3).

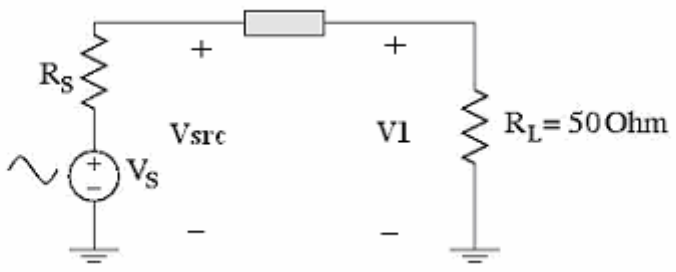

Figure 3.4.2 The schematic of basic true time delay circuit

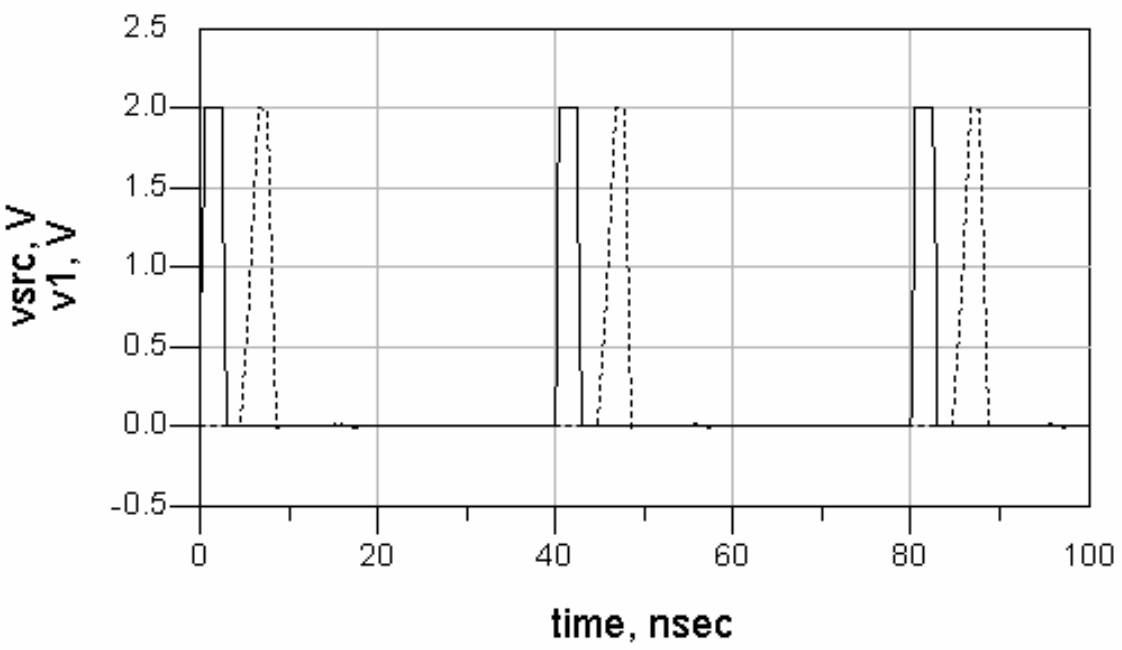

Figure 3.4.3 The simulation results of the basic transmission line delay circuit

These transmission lines are also used as the delay elements of the phase shifter circuit; the lengths and numbers of the microstrip transmission lines are selected in accordance with the desired pulse widths and resolution since the microstrip transmission line lengths determine the amount of time delay. The characteristic impedance of the microstrip transmission lines is important and has to be adjusted to the impedance of the other components in the system since the transmission lines directly affect the impedance matching of the circuit. Otherwise, the reflections occur on the transmission lines. For instance, in **Figure 3.4.4(a)**, the circuit generates a Gaussian monocycle at the output from the input mono-pulse signal by using phase shifter circuit with short circuit stub with the transmission line. The pulse generator circuit is simulated for two different conditions of characteristic impedance of the transmission line: matched and mismatched with the output impedance. In the first case, a smooth monocycle is produced at the output as shown in **Figure 3.4.4(b)**. In the figure, no reflection and overlapping take place so that it can be said that the length and width of the transmission line are correctly set. However, in latter case, the impedance of the transmission line at the phase shifter circuit is not equivalent to the output impedance (R_L) in order that the output signal is distorted by the reflections by reason of the impedance mismatching as shown in **Figure 3.4.4(c)**. Therefore, distinguishing the monocycle from the graph becomes impossible.

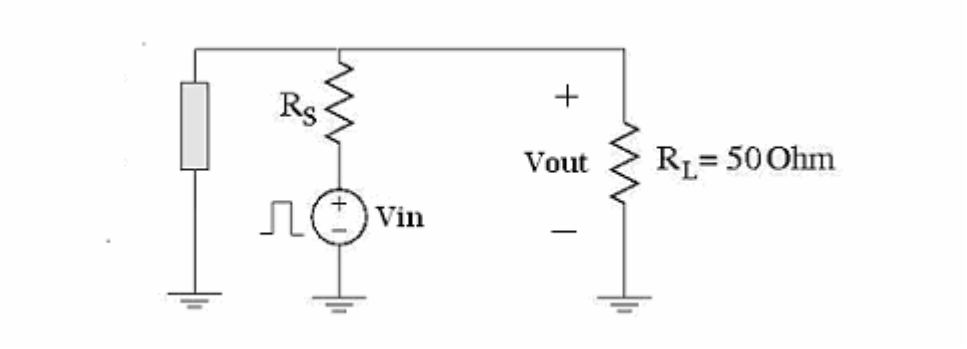

(a)

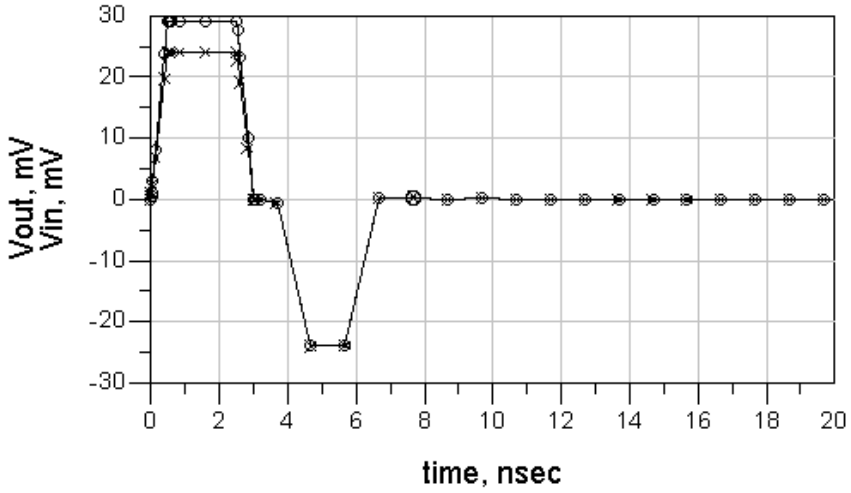

(b)

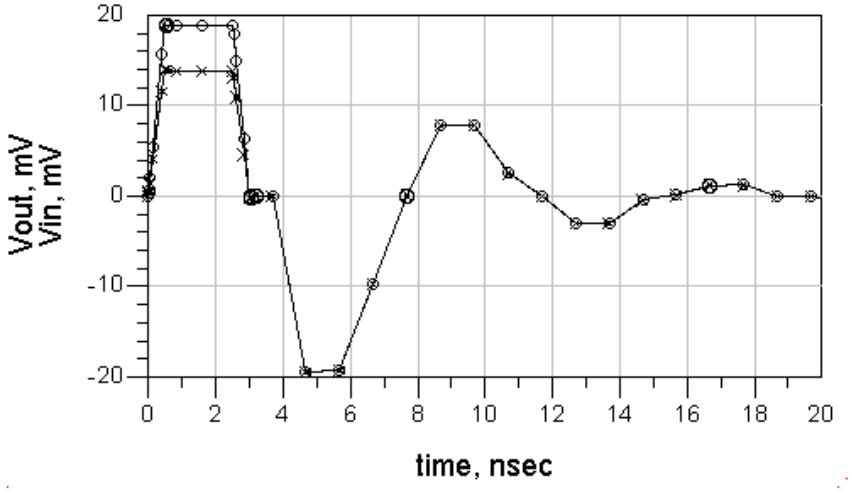

(c)

Figure 3.4.4 (a) Schematic of the Monocycle generator circuit (**b**) Simulation result of output signal in (a) with matched short circuit stub (**c**) Simulation result of output signal in (a) with mismatched short circuit stub

3.4.3 PIN Diodes and High Frequency Switches

Other important components of the phase shifter circuit are PIN diodes. PIN diodes find applications as high-frequency switches for RF signals up to 50 GHz. They contain an additional layer of an intrinsic (I-layer) or lightly doped semiconductor sandwiched between highly doped p^+ and n^+ layers as shown in **Figure 3.4.5**.

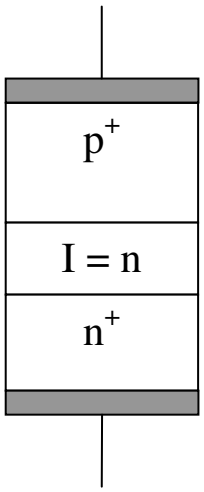

Figure 3.4.5 Simplified structure of a PIN diode

Depending upon application and frequency range, the thickness of the middle layer ranges from 1 to 100 µm. In forward direction, the diode behaves as if it possesses a variable resistance controlled by the applied current. However, in reverse direction the lightly doped inner layer creates space charges whose extent reaches the highly doped outer layers. This effect takes place even for small reverse voltages and remains essentially constant up to high voltages, with the consequence that the diode behaves similar to a dual plate capacitor [17]. The bias point setting required to operate the PIN diode has to be provided through a DC circuit that must be separated from the RF signal path. The DC isolation is achieved by a radio frequency coil (RFC) or RF choke, representing a short circuit at DC and an open circuit at high frequency. Conversely, DC blocking capacitors (C_{BL}) represent an open circuit at DC and a short circuit at RF. **Figure 3.4.6** shows a typical switching circuit where the PIN diode is used in series connection.

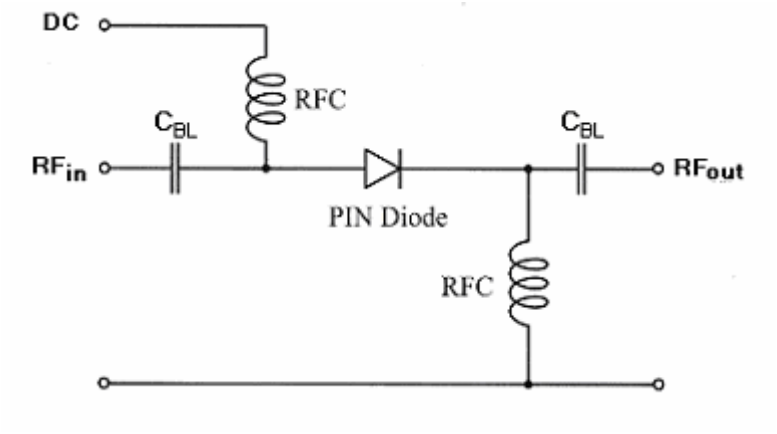

Figure 3.4.6 Switching circuit with biased PIN diode in series configuration

3.4.4 PIN Diodes/Transmission Line Sub-section

In the phase shifter circuit, the PIN diodes are used as RF switch to control whether the signal goes through that delay element (transmission line) or not. In each PIN diodes/transmission line sub-section, there are three PIN diodes. As shown in **Figure 3.2.1**, if the series PIN 1 diode is forward-biased with positive bias voltage, then the PIN 2 and 3 are reverse biased, and hence the RF signal reaches the point B from the point A over the PIN 1 diode. On the other hand, if the PIN 2 and 3 are forward biased with negative voltage, then the PIN 1 diode is reverse-biased and the RF signal reaches the point B from the point A over the transmission line, and is delayed by the transmission line length. Depending on the desired pulse width, one or more phase shifter sections may be connected in series. Using DC blocking capacitors connected between the adjacent phase shifter sections can capacitively couple all these phase shifter sections. Various combinations of the PIN diodes can be used to obtain 2^N different durations by using only N phase shifter sections.

3.4.5 Prevention of the Reflections over Transmission Line

The series PIN diodes to the transmission lines also avoids undesired reflections during the pulse generation. In the early design of the pulse generator, the series diodes to the transmission lines were not employed as shown in **Figure 3.4.7(a)**. In the

simulations, when the PIN diode parallel to the transmission line is turned off, the mono-pulse is generated with the desired pulse width as shown in **Figure 3.4.7(b)**; however, when the diode is turned on, the current flows over both the PIN diode and the transmission line. As a result at the output of the generator, distorted signal occurs as shown in **Figure 3.4.7(c)**. When the number of sections in the phase shifter circuit are increased, the distortion becomes severe and the affects the all results.

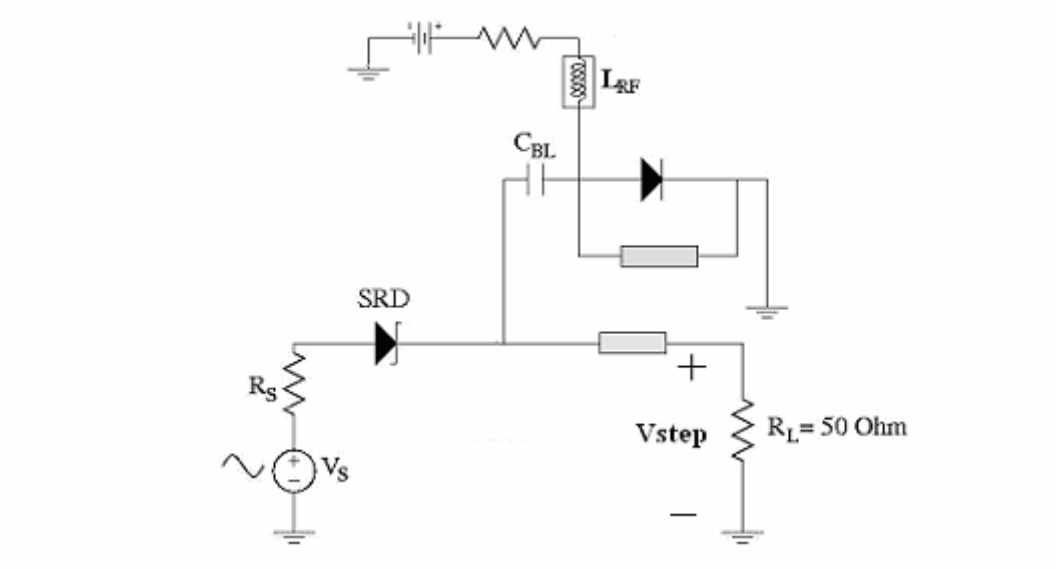

(a)

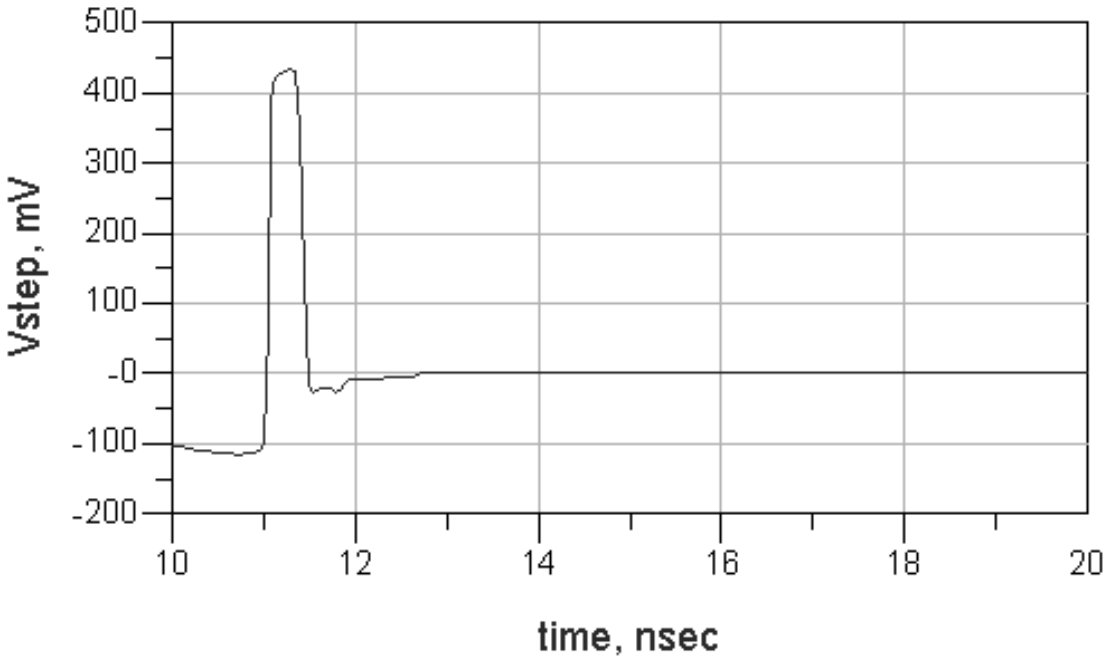

(b)

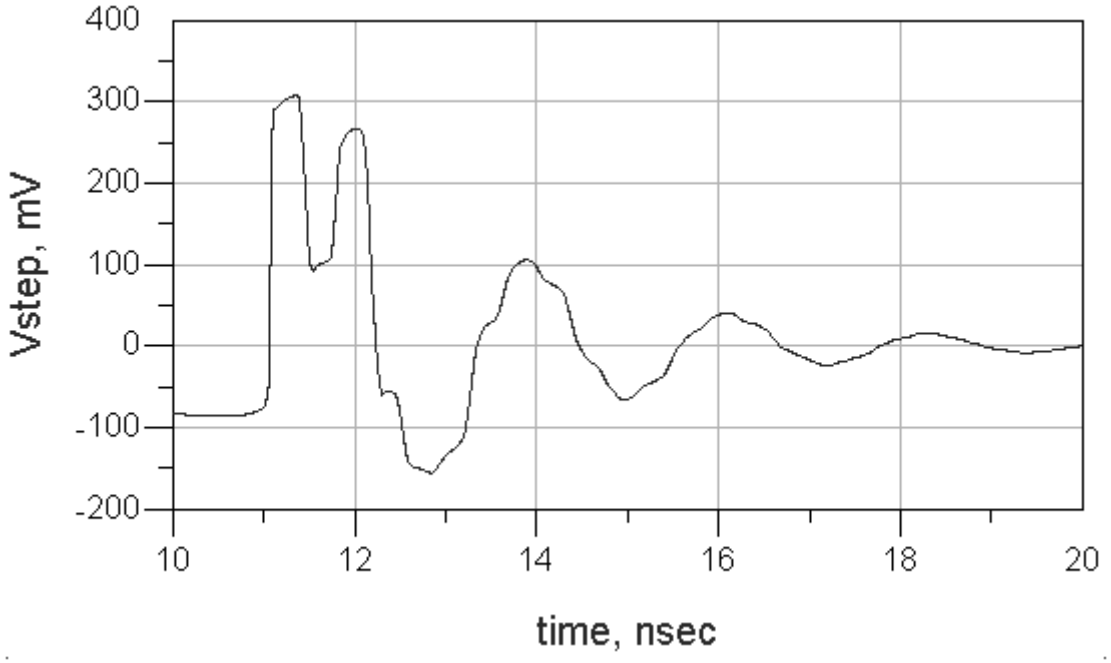

(c)

Figure 3.4.7 (a) Schematic of the Single-Bit Tunable UWB Pulse Generator (**b)** Simulation result of forward bias in the ADS **(c)** Simulation result of reverse bias

In order to prevent the multiple reflections over the transmission line, additional PIN diodes are connected to the transmission line with different combinations. In **Figure 3.4.8** and **Figure 3.4.9**, all connection combinations of the series PIN diodes and the simulation results are shown. In **Figure 3.4.8(a)** and **Figure 3.4.9(a)**, additional PIN diodes are connected to the each side of the transmission line. They both decrease the reflections as shown in **Figure 3.4.8(b)** and **Figure 3.4.9(b)**; however, they do not avoid the all reflections since the reflections still occurs at the sides which the diodes are not connected. The reflections have same polarities with the desired pulse since the transmission line behaves like an open circuit stub due to the PIN diode at one side. Therefore, in order to avoid the reflections, the PIN diodes should be connected to the both sides of the transmission lines in the same direction with each other and in the opposite direction with the parallel PIN diode as shown in **Figure 3.4.10(a)**. No reflection occurs in the simulation result in **Figure 3.4.10(b)**

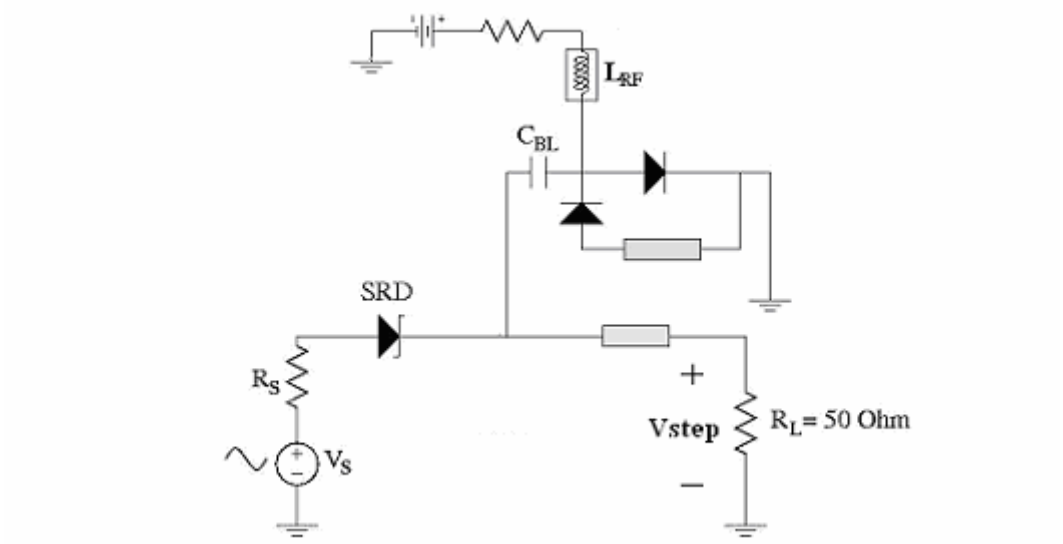

(a)

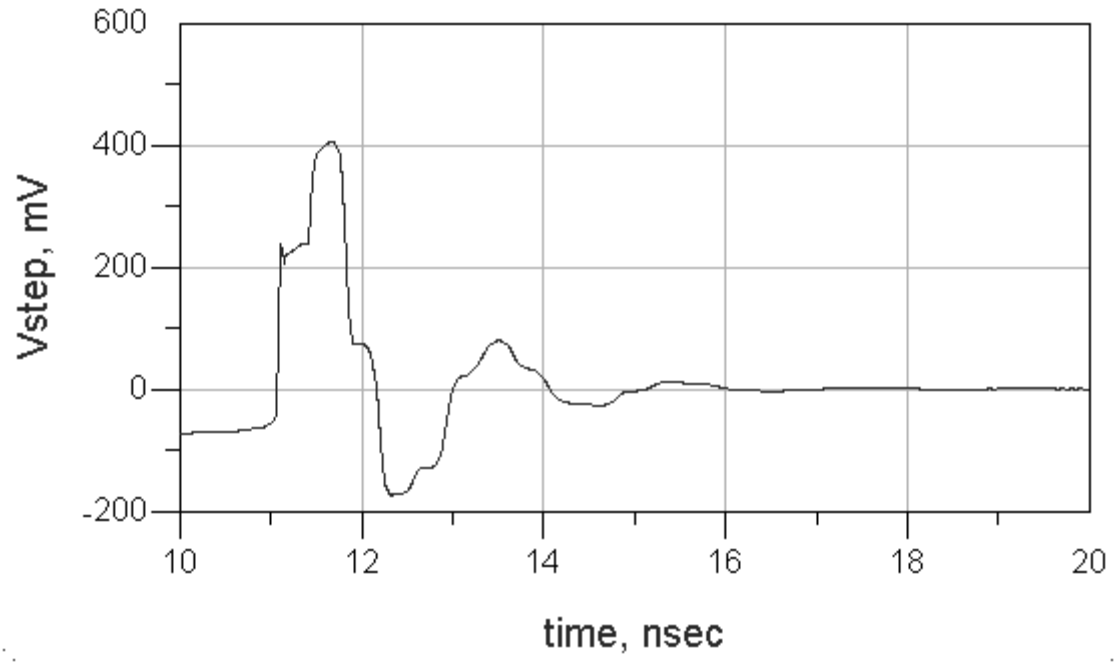

(b)

Figure 3.4.8 (a) Schematic of the Single-Bit Tunable UWB Pulse Generator with series PIN diode at left side of transmission line **(b)** Simulated Pulse width of the circuit in (a)

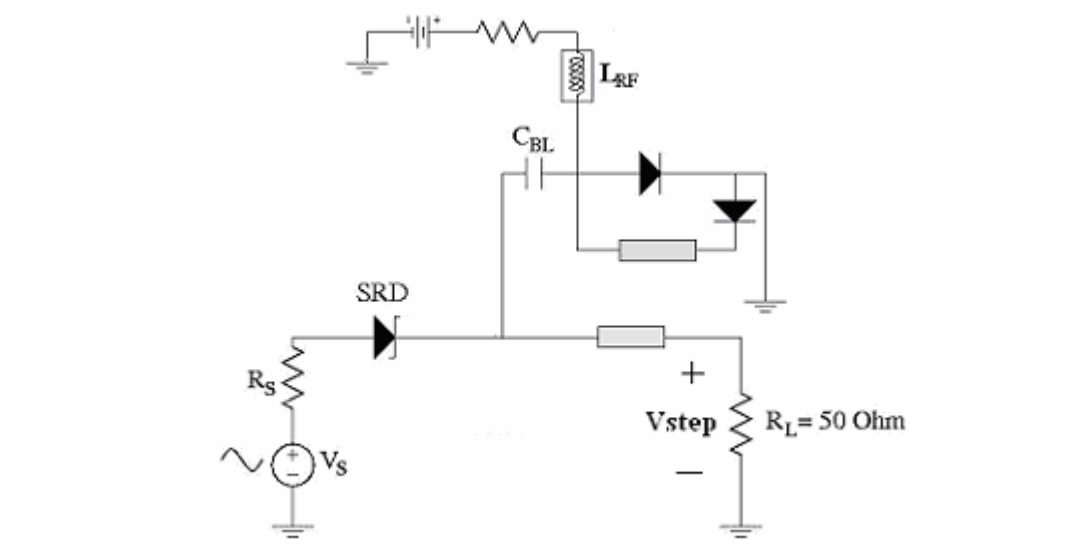

(a)

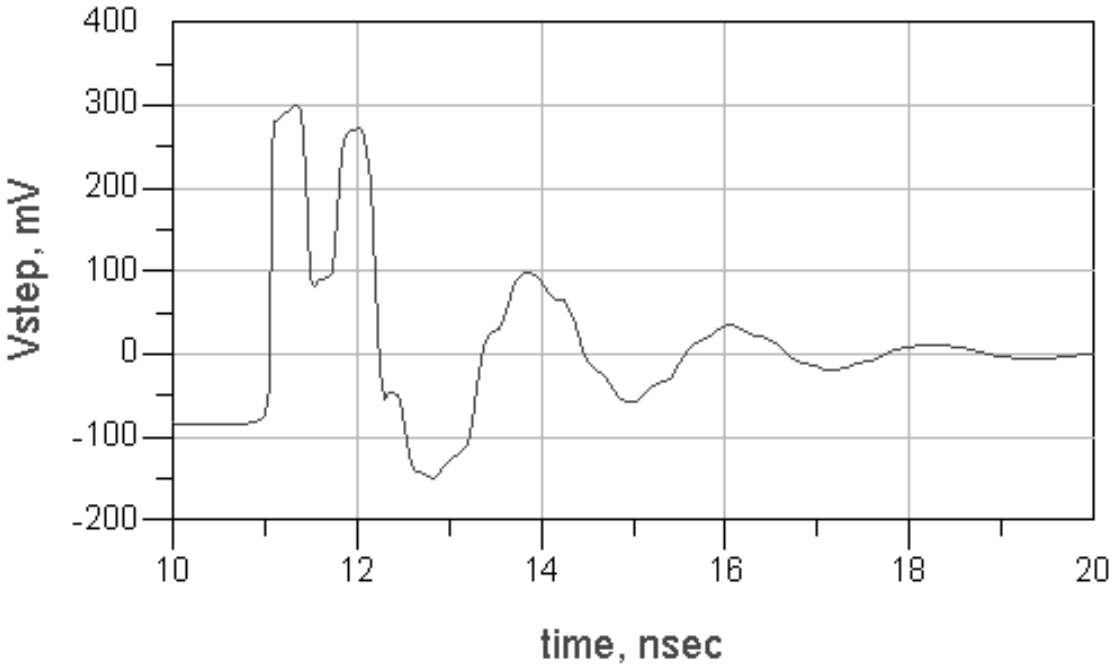

(b)

Figure 3.4.9 (a) Schematic of the Single-Bit Tunable UWB Pulse Generator with series PIN diode at right side of transmission line **(a)** Simulated Pulse width of the circuit in (a)

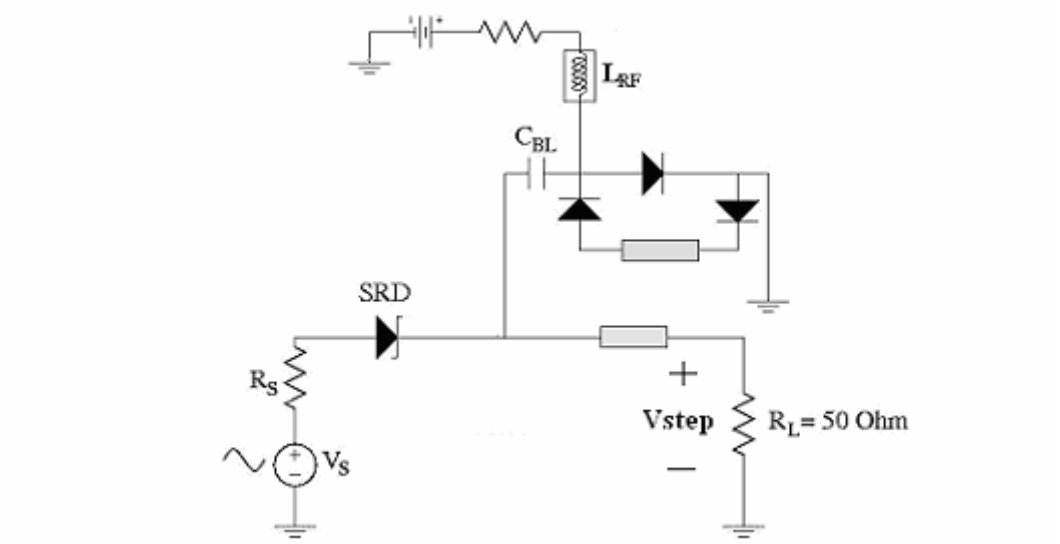

(a)

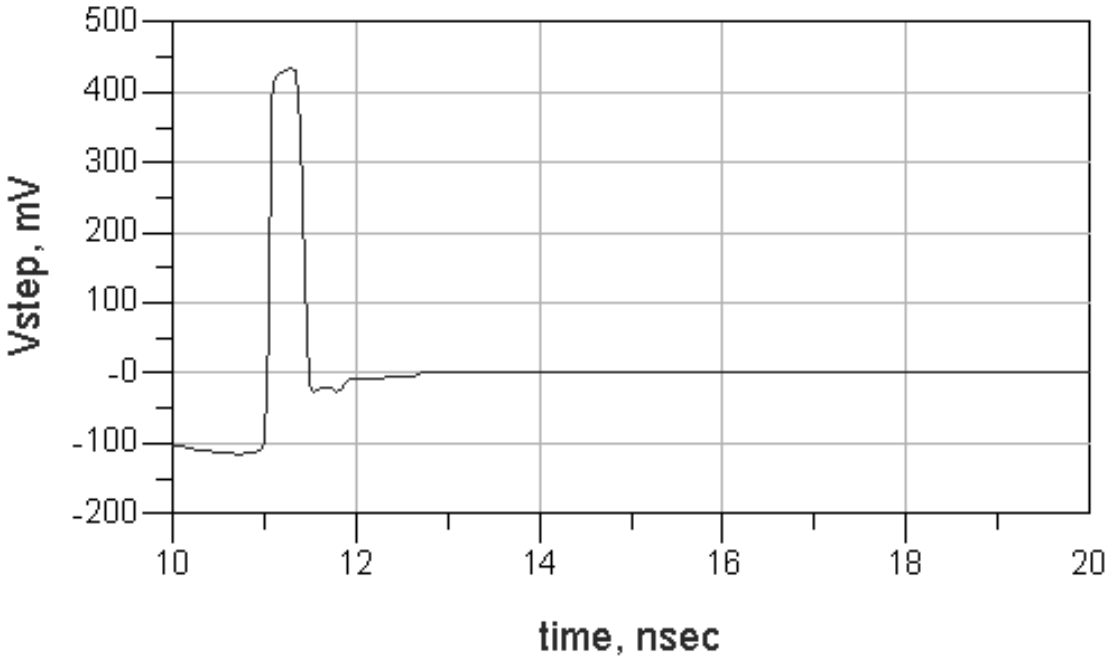

(b)

Figure 3.4.10 (a) Schematic of the Single-Bit Tunable UWB Pulse Generator with series PIN diodes at both sides **(b)** Simulated Pulse width of the circuit

As shown in the **Figure 3.4.10**, there is no reflection over the single-bit tunable pulse generator. In the N-bit digitally tunable pulse generator, each of the N PIN diodes/transmission line sub-sections in the parallel short circuit stub is biased and controlled independently. Therefore, no reflection still occurs while N sub-sections, in the **Figure 3.4.10,** are connected in series.

4. SIMULATION RESULTS AND MEASUREMENTS

This chapter contains the results and discussions of simulations result carried out at Agilent Advanced Design System (ADS) platform and experiments carried out at the RF/Wireless Communication and Optoelectronic Research Laboratories of Sabancı University during the studies of this thesis. Two different versions of generator circuit have been designed and realized with microstrip technology on a high frequency substrate for performance comparison. In this chapter, the measurement setups, simulations results and measurement results are given in details.

4.1 SIMULATION AND MEASUREMENT SETUPS

Both 2-section and 4-section versions of the N-bit digitally tunable UWB pulse generator have been designed and simulated using Agilent ADS version 2003c to compare their pulse generation and frequency bandwidth performances. The overall schematic of the 2-bit digitally tunable UWB pulse generator is shown in the **Figure 4.1.1**. In the figure, the transmission lines are implemented using microstrip line technology, thus the widths of the transmission lines are adjusted to:

$$\frac{W}{d} = \begin{cases} \dfrac{8e^{A}}{e^{2A}-2} & \text{for } \dfrac{W}{d} < 2 \end{cases} \qquad \text{where} \quad A = \frac{Z_0}{60}\sqrt{\frac{\varepsilon_r+1}{2}} + \frac{\varepsilon_r-1}{\varepsilon_r+1}\left(0.23+\frac{0.11}{\varepsilon_r}\right)$$

$$A = \frac{50}{60}\sqrt{\frac{4.55+1}{2}} + \frac{4.55-1}{4.55+1}\left(0.23+\frac{0.11}{4.55}\right) \approx 1.51$$

$$\frac{W}{d} = \frac{8e^{A}}{e^{2A}-2} = \frac{8e^{1.52}}{e^{2(1.52)}-2} = 1.92 \quad \Rightarrow \quad W = 1.92x1.55 \approx 3mm$$

3 mm for matching the transmission lines to the 50 Ohm at working frequencies by using equation 3.5 in the Chapter 3. The lengths of the transmission lines at the phase shifter circuit are selected as:

$$\frac{d}{W} = \frac{1.55}{3} = 0.52$$

$$\varepsilon_e = \frac{\varepsilon_r + 1}{2} + \frac{\varepsilon_r - 1}{2}\frac{1}{\sqrt{1+12\frac{d}{W}}} = \frac{4.55+1}{2} + \frac{4.55-1}{2}\frac{1}{\sqrt{1+12\times 0.52}} = 3.45$$

$$v_p = \frac{c}{\sqrt{\varepsilon_e}} = \frac{3x10^8}{\sqrt{3.45}} = 1.6x10^8\, m/\sec$$

$$l = \Delta t \times v_p = 200x10^{-12}\times 1.6x10^8 = 3.2cm \approx 3cm \qquad for\ \ 200p\sec$$

$$= 400x10^{-12}\times 1.6x10^8 = 6.4cm \approx 6cm \qquad for\ \ 400p\sec$$

3 and 6 cm to produce 200 and 400 psec delays which are calculated by using equations 3.1 and 3.3, respectively. On the ADS platform, the transient simulation of the pulse generator is carried out between 0 to 50 nsec with 50 psec steps; the substrate on which the circuit is implemented is defined infinitely large and dielectric properties, the thickness and the dielectric constant, of the substrate are adjusted to FR4 glass epoxy.

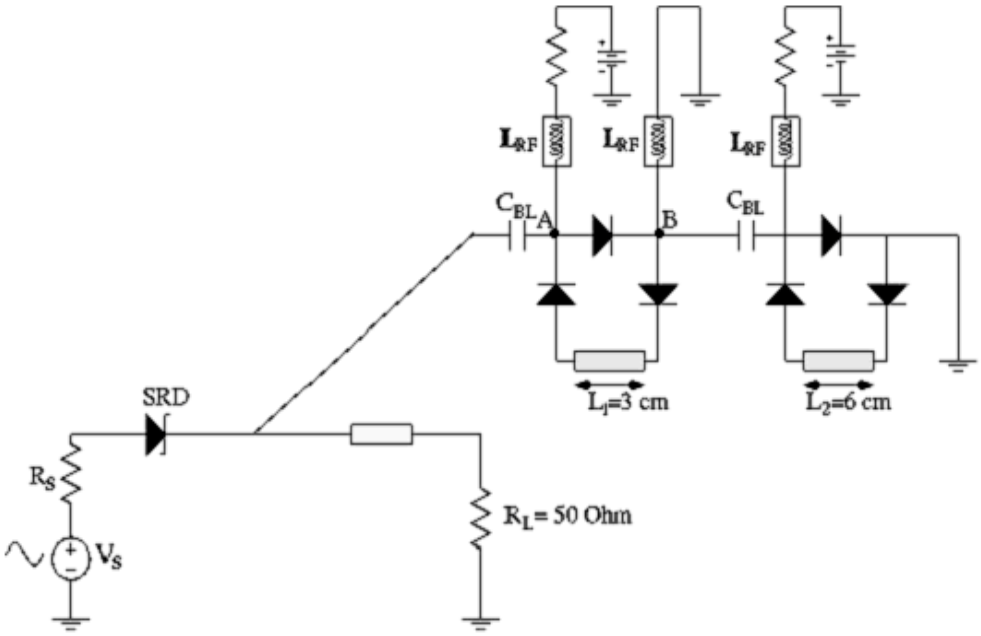

Figure 4.1.1 Schematic of the 2-bit digitally tunable UWB pulse generator

In the 4-bit digitally tunable UWB pulse generator, the transmission lines are also implemented using microstrip line technology, the widths of the transmission lines are adjusted to 3 mm since the 4-bit UWB pulse generator is presumed to work at the same frequency with the 2-bit version and the lengths of the transmission lines are selected as:

$$\begin{aligned} l = \Delta t \times v_p &= 50x10^{-12} \times 1.6x10^{8} = 0.8cm \approx 0.75cm && for \;\; 50p\,\text{sec} \\ &= 100x10^{-12} \times 1.6x10^{8} = 1.6cm \approx 1.5cm && for \;\; 100p\,\text{sec} \\ &= 200x10^{-12} \times 1.6x10^{8} = 3.2cm \approx 3cm && for \;\; 200p\,\text{sec} \\ &= 400x10^{-12} \times 1.6x10^{8} = 6.4cm \approx 6cm && for \;\; 400p\,\text{sec} \end{aligned}$$

0.75, 1.5, 3 and 6 cm shown in the **Figure 4.1.2** to produce 50, 100, 200 and 400 psec delays, respectively. In order to constitute the 4-bit UWB pulse generator two additional PIN diodes/transmission line sub-sections have been attached to the end of phase shifter circuit of the 2-bit UWB pulse generator. The numbers of output pulses are increased from 4 (2^2) to 16 (2^4).

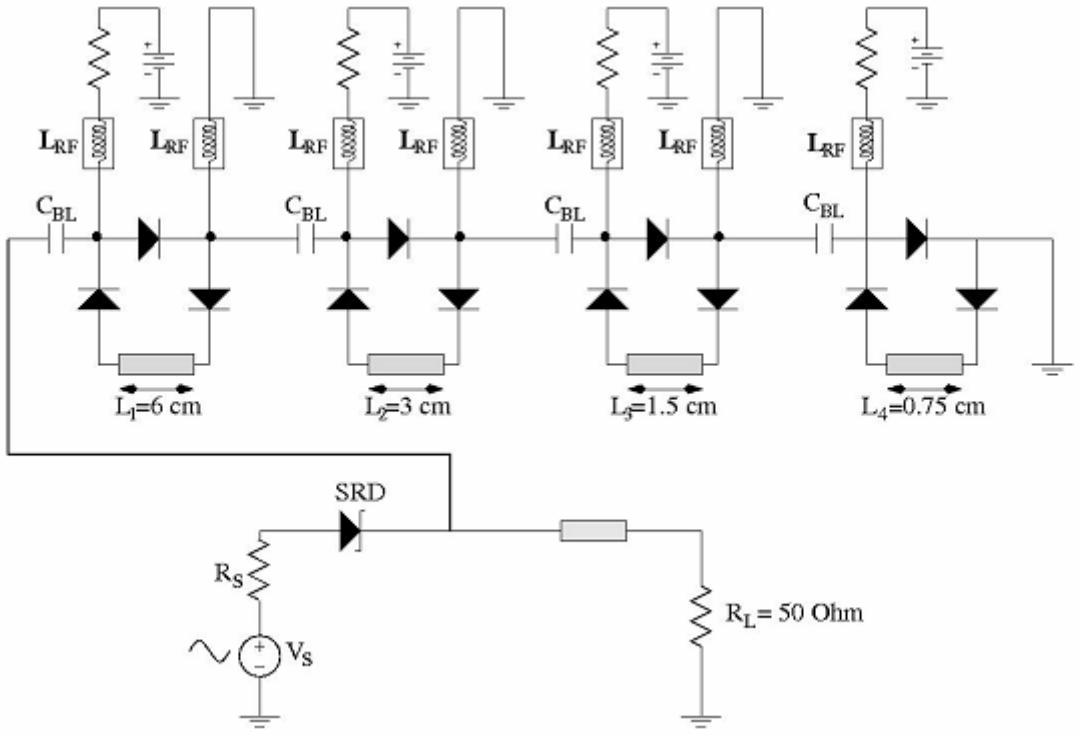

Figure 4.1.2 Schematic of the 4-bit digitally tunable UWB pulse generator

After achieving the adequate proposed specifications in the simulation results, the UWB pulse generator circuits have been implemented on the FR-4 glass epoxy high frequency substrate with relative dielectric constant of 4.55 and thickness of 1.55 mm which can work up to 4-5 GHz. In the **Figure 4.1.3** and **Figure 4.1.4**, the implemented circuits are shown; the SRDs used in the circuits are MSD700 series glass packaged diodes with low transition times and high efficiencies. The PIN diodes are ultra-fast switching low-high power MMP7010 series diodes with high temperature passivation for reliability and grown junction for sharp "I" region interface features. Both diodes are manufactured by Micrometrics Inc. The datasheets and electrical characteristics of the components are given in the **Appendix B**.

To obtain the desired pulse widths at the outputs, two and four PIN diodes/transmission line sub-sections are used in the phase shifter circuits of the pulse generators. In order to separate switches of the adjacent sub-sections, 0.1 μF DC blocking chip capacitors are situated among the sub-sections and to prevent the reflection at the bias DC and ground very wide-band surface mount ADCH-80 series RF chokes of Mini-Circuits company are employed. Inductance value of the RF choke is varied by DC current so that the inductance could be nearly 1.5 μH at 20 mA in our pulse generator circuits.

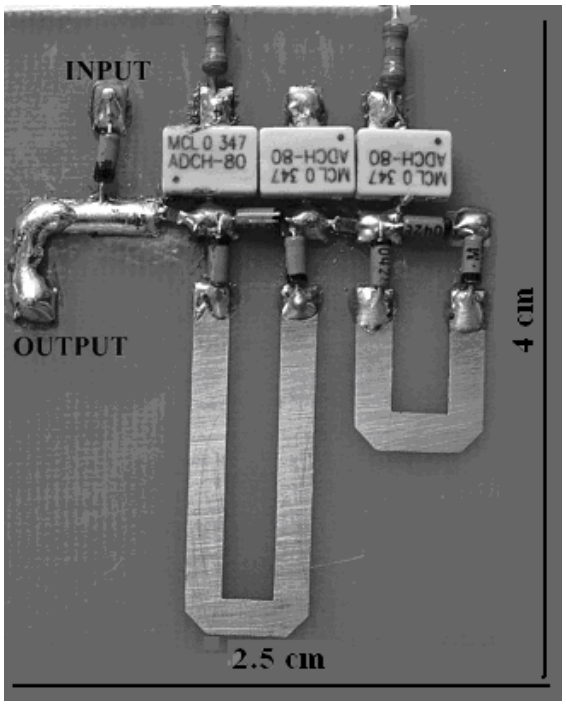

Figure 4.1.3 The 2-bit digitally tunable UWB pulse generator

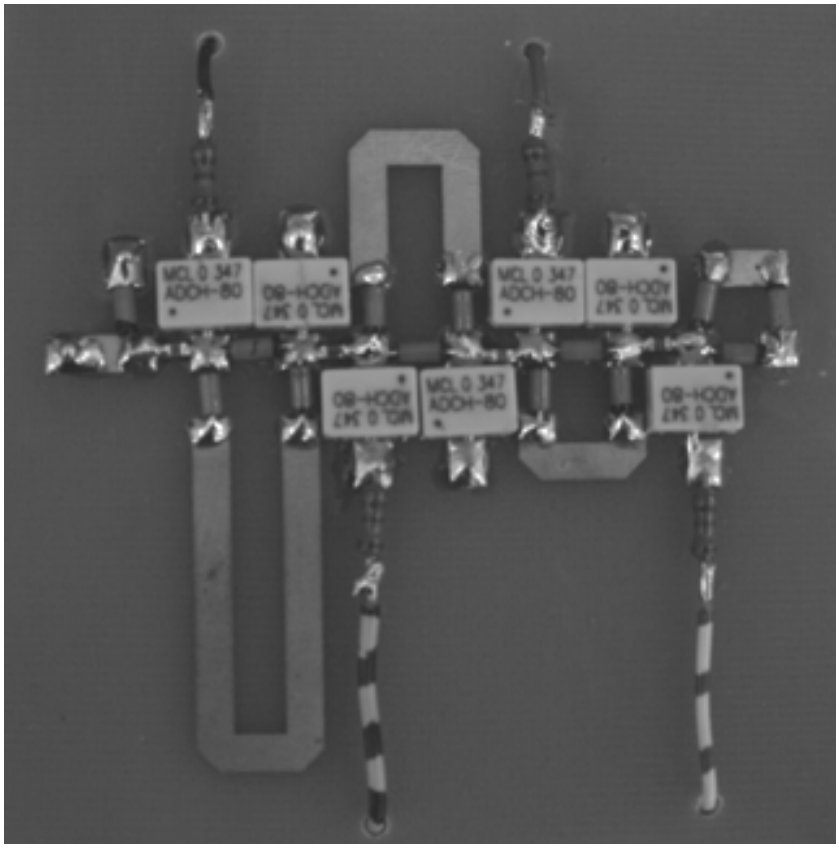

Figure 4.1.4 The 4-bit digitally tunable UWB pulse generator

4.2 LIMITATIONS AND PROBLEMS OF THE CIRCUITS

In the circuits, electrical characteristics of the components and the implementation conditions cause some problems at working performance. For instance, additional transmission lines are placed between the capacitors and the PIN diodes in order to solder the components that increase the pulse widths. Therefore, new modifications become necessary to afford the specifications. However, the major limitations in the pulse generation are the transition time of the SRD and the group delay of the PIN diodes and the DC blocking capacitors. In order to measure the limitations of the components and the circuits, two different measurement techniques both in time and frequency domain are used. The techniques are explained in the following sections in detail.

4.2.1 Maximum Transition Time of the SRD

The minimum pulse width that can be obtained by the pulse generator circuits is limited by the SRD's maximum transition time, which is measured by Agilent 8722ES Vector network analyzer and was found to be around 125 psec. In the network analyzer, the slope of the phase measurement of the SRD is the rise time of the sharp edge, which is 125 psec. **Figure 4.2.1** shows the measurement result of the circuit when all sub-sections of the phase shifter circuit are biased with 0 Volts. Therefore, all PIN diodes turn off and the sinusoidal signal only passes through the SRD between input and output ports.

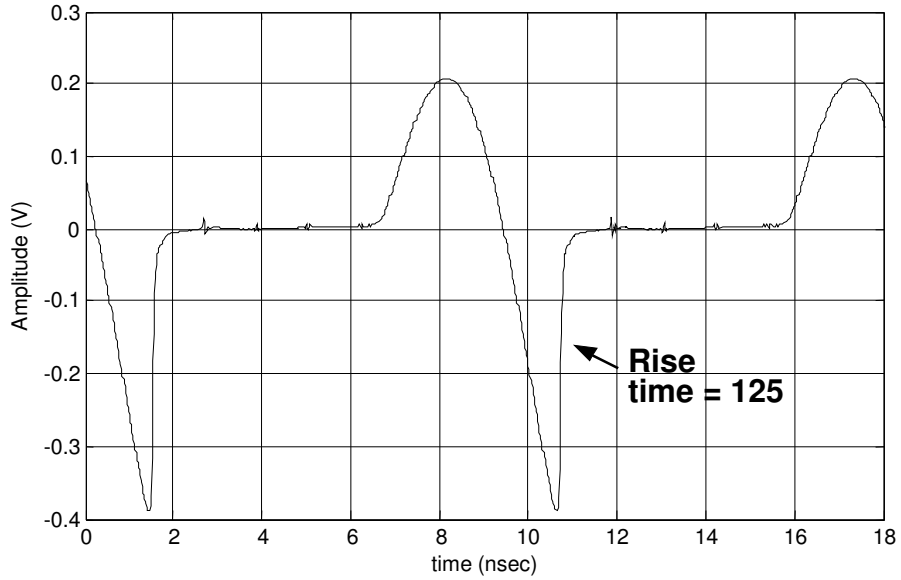

Figure 4.2.1 The rise time of the sharp edge generated by SRD measured by 86100C

4.2.2 The Group Delay of the PIN Diodes and DC Blocking Capacitors

In addition, the group delays of the PIN diodes and the DC blocking capacitors will also affect the pulse width. The group delay of one section of the series PIN diode switch shown in the **Figure 4.1.1** is measured with by network analyzer at forward bias and gives rise to a time delay of 110 psec which can be calculated from the **Figure 4.2.2** as slope of the phase component of the reflection coefficient, S_{11}. Note that the overall pulse width is affected by twice the amount of group delay of the PIN diodes and the dc blocking capacitors since the UWB pulse goes over the PIN diodes and then reflected by the short circuit, and goes over the PIN diodes once again to reach the load.

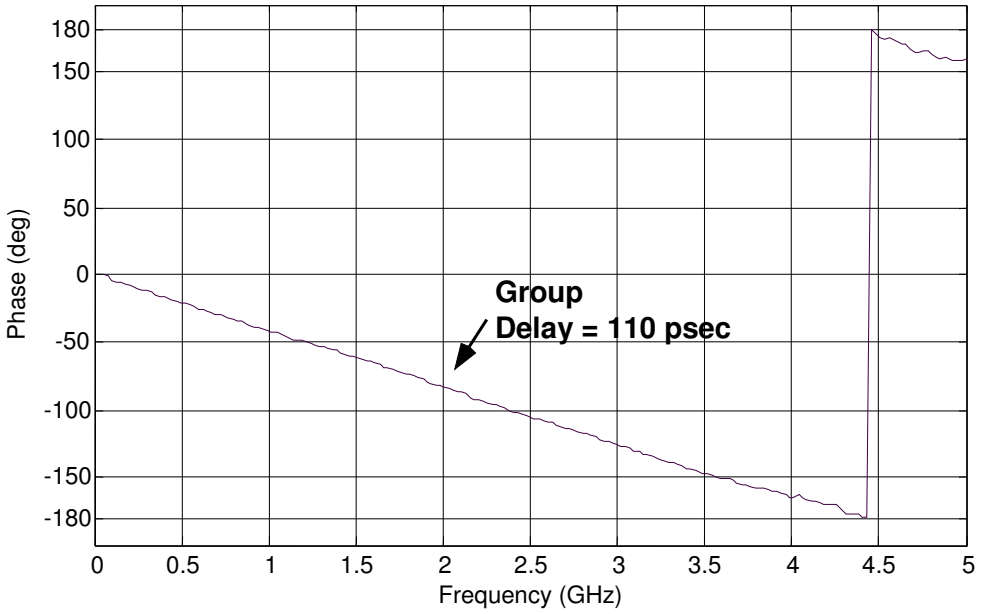

Figure 4.2.2 Phase of S_{11} versus frequency graph of the series PIN-diodes measured by 8722ES

Therefore, with regard to the limitations of the circuit, the possible shortest pulse width durations are around 550 and 900 psec for 2-bit and 4-bit pulse generator, respectively; only including the offset delay of SRDs' maximum transition times, the group delays of PIN diodes and DC blocking capacitors and the extra delays due to additional transmission lines. The possible shortest pulse width duration of 4-bit pulse generator is greater than the duration of 2-bit pulse generator since the number of the PIN diodes and DC blocking capacitors and the additional transmission lines are more than the 2-bit pulse generator.

4.3 OUTPUT PULSE WIDTHS OF THE GENERATOR CIRCUITS

The output pulse durations of the generators are dependent on the limitations of the diodes and capacitors and the chosen lengths of the transmission (delay) lines. The shortest pulse width durations are the cumulative of the limitations as mentioned above. The other pulse widths ascend with the steps of delay lines. In 2-bit digitally tunable pulse generator, the steps of delay lines are adjusted to the 400 psec and in the 4-bit digitally tunable pulse generator; the steps are adjusted to the 100 psec to increase the

sensitivity of the resolution. Therefore, the possible pulse durations with respect to the limitations and the steps of delay lines are given in the **Table 1** and **Table 2** with their digital codes. As mentioned in chapter 3, the all sub-sections can be controlled independently to get 2^N pulses with different pulse widths. Code 0 means that the sub-section is biased with -5 Volts and the series PIN diode is forward-biased in the sub-section so that signal goes through the series PIN diode. Code 1 means that the sub-section is biased with 5 Volts and the series PIN diode is reversed-biased in the section so that the signal goes through the transmission line.

Code		**Pulse Width (psec)**
Sub-Section 1	**Sub-Section 2**	
0	0	550
0	1	950
1	0	1350
1	1	1750

Table 4.3.1 Pulse durations of 2-bit digitally tunable pulse generator that can be generated by different biasing conditions of the phase shifter sections

Code				Pulse Width (psec)
Sub-Section 1	**Sub-Section 2**	**Sub-Section 3**	**Sub-Section 4**	
0	0	0	0	900
0	0	0	1	1000
0	0	1	0	1100
0	0	1	1	1200
0	1	0	0	1300
0	1	0	1	1400
0	1	1	0	1500
0	1	1	1	1600
1	0	0	0	1700
1	0	0	1	1800
1	0	1	0	1900
1	0	1	1	2000
1	1	0	0	2100
1	1	0	1	2200
1	1	1	0	2300
1	1	1	1	2400

Table 4.3.2 Possible pulse durations of 4-bit digitally tunable pulse generator

4.4 2-BIT DIGITALLY TUNABLE UWB PULSE GENERATOR

4.4.1 Simulation Results

The ADS simulated output pulses of the 2-Bit digitally tunable UWB pulse generator are shown in **Figure 4.4.1**. The graphs show the pulse widths ranging from 550 psec to 1750 psec with steps of 400 psec that corresponds to frequency bandwidth of 550 MHz to 1.8 GHz. Amplitudes of the pulse output are around 400 mV when the applied input has a peak of 1.4 V at a pulse repetition frequency of 20 MHz. Also, note that the residual of the 20 MHz input signal around 28-31 nsec, which can easily be removed by a simple high pass filter.

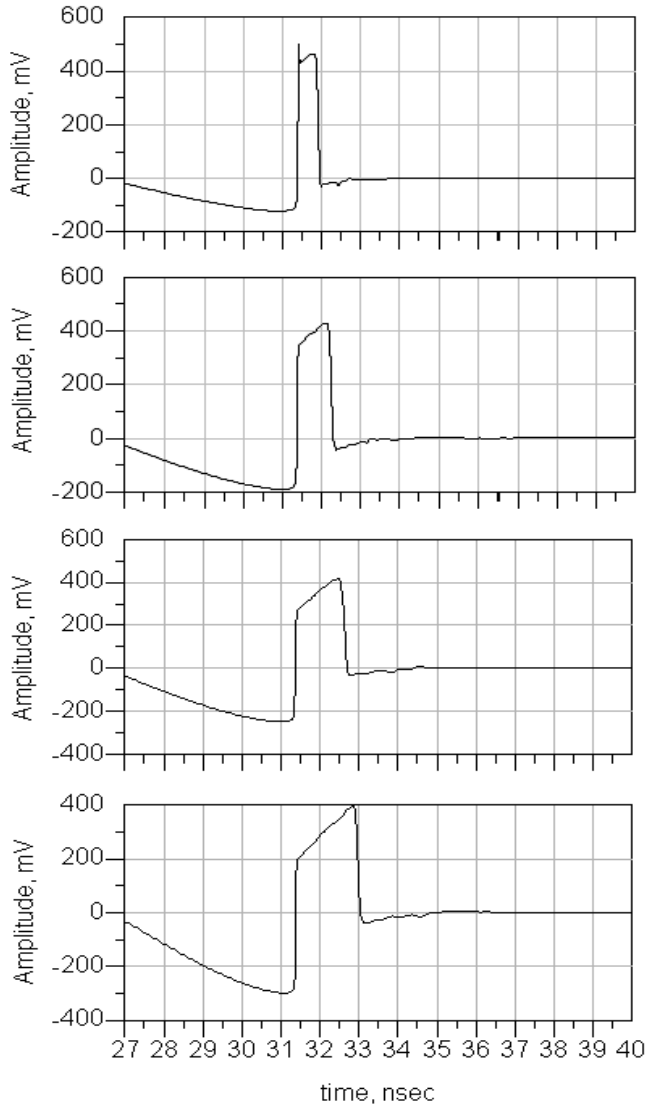

Figure 4.4.1 The ADS simulated pulses of 2-Bit digitally tunable UWB pulse generator

4.4.2 Measurement Results

The overall measurement setup is shown in **Figure 4.4.2**. To capture the generated narrow pulses, measurements are done with Agilent 86100C Digital Communication Analyzer that can work up to 20 GHz. The 20 MHz function waveform generator is selected since input sinusoidal signal at 20 MHz is enough to produce UWB pulses. Each PIN diode switch is controlled with a DC power supply; in accordance with the states of the switches, the DC power supply produces 5 or -5 Volts for biasing. The experimental results of the UWB pulse generation are shown in **Figure 4.4.3**, where the all possible combinations are plotted on the graphs from the shortest one to the longest one. The amplitudes of the pulses are around 300 mV for an applied signal of 1.4 V at the same frequency of 20 MHz. The pulse widths are also in very good agreement with the simulations for 550 psec to 1750 psec duration pulses. In the measurement, the residual of the 20 MHz input signal is also observed before the generated pulses and as mentioned in the simulation results that can be easily removed by a high pass filter, which is shown in the 4-bit UWB pulse generator.

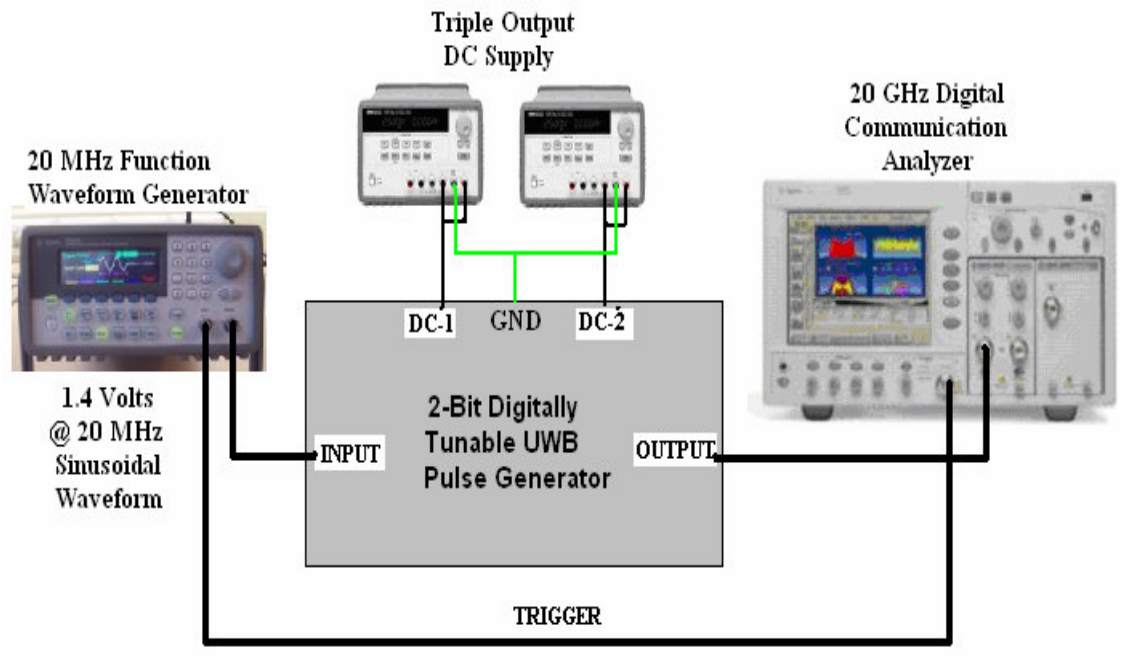

Figure 4.4.2 The overall measurement setup of the 2-bit Digitally Tunable UWB Pulse Generator

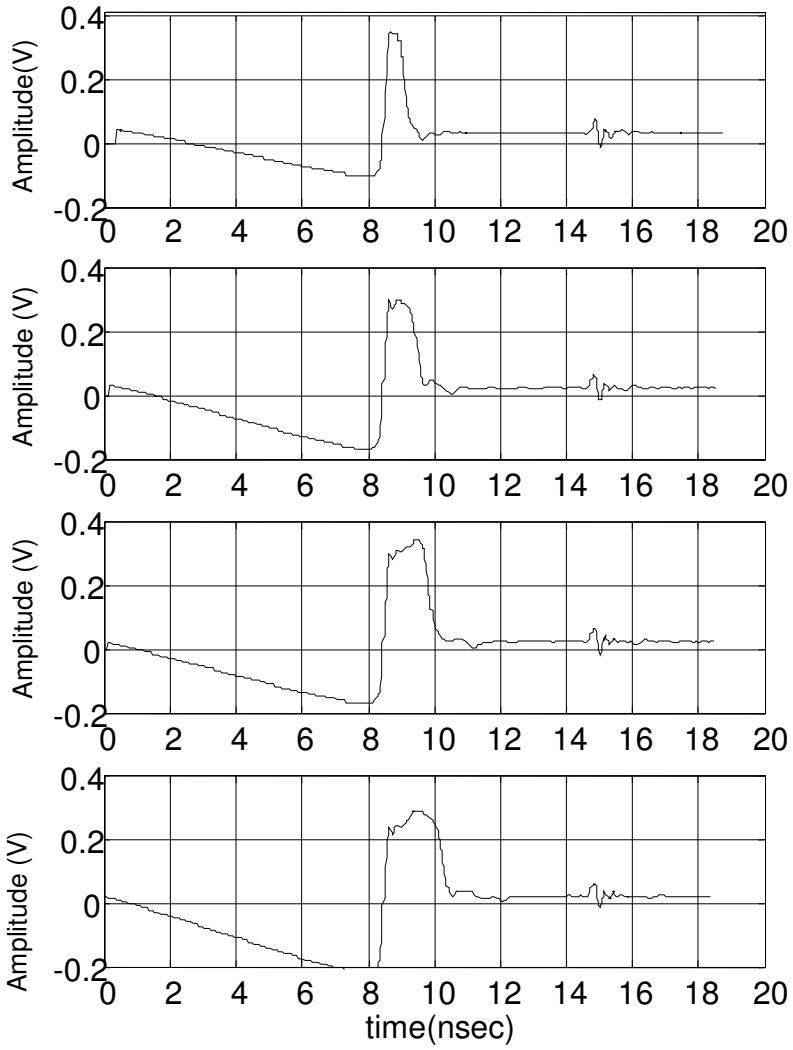

Figure 4.4.3 Variable width pulses generated by UWB pulse generator circuit (measured)

4.4.3 Measurement Results in Frequency Domain

The working principles and the technology of the 2-bit digitally tunable UWB pulse generator are explained by Yilmaz, et.al [18]. The frequency domain characteristics of the circuit are obtained by taking the Fourier transform of the measured pulses in time domain. The frequency domain characteristics of the longest and shortest pulses are shown in **Figure 4.4.4**, where the longest pulse has a first null bandwidth of 600 MHz, and the shortest pulse has first null bandwidth of 1800 MHz,

respectively. The measurements are proved that the 2-bit digitally tunable pulse generator is suitable for applications working between 600 MHz and 1800 MHz.

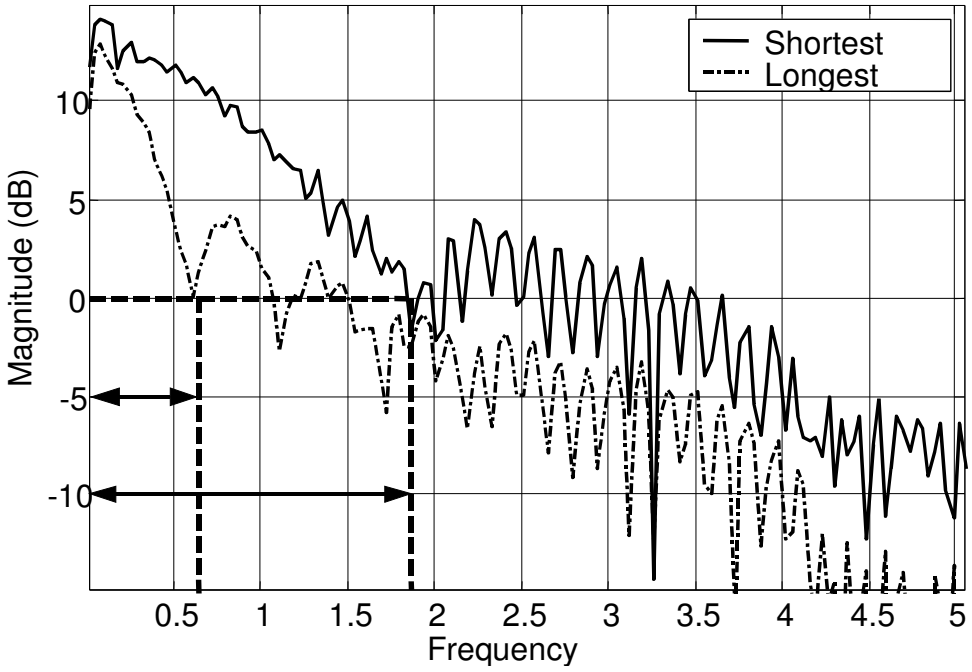

Figure 4.4.4 Frequency Domain Characteristics of the longest and shortest pulses

4.5 4-BIT DIGITALLY TUNABLE UWB PULSE GENERATOR

4.5.1 Simulation Results

The 4-bit version of the UWB pulse generator is also simulated on ADS platform. The output pulses ranges from 900 psec to 2400 psec with steps of 100 psec that corresponds to frequency bandwidth of 420 MHz to 1.2 GHz. The minimum pulse width increases to the 900 psec since the whole group delays of the PIN diodes and DC blocking capacitors ascend when the numbers of sub-sections in the phase shifter circuit increase. Simulation results of the circuit are shown in **Figure 4.5.1**. Although only the pulses with codes 0000, 0100, 1000, and 1111 are demonstrated in the figure, the circuit can generate 16 pulses with different pulse width. Using a high pass filter in the simulations eliminates the residual of low frequencies.

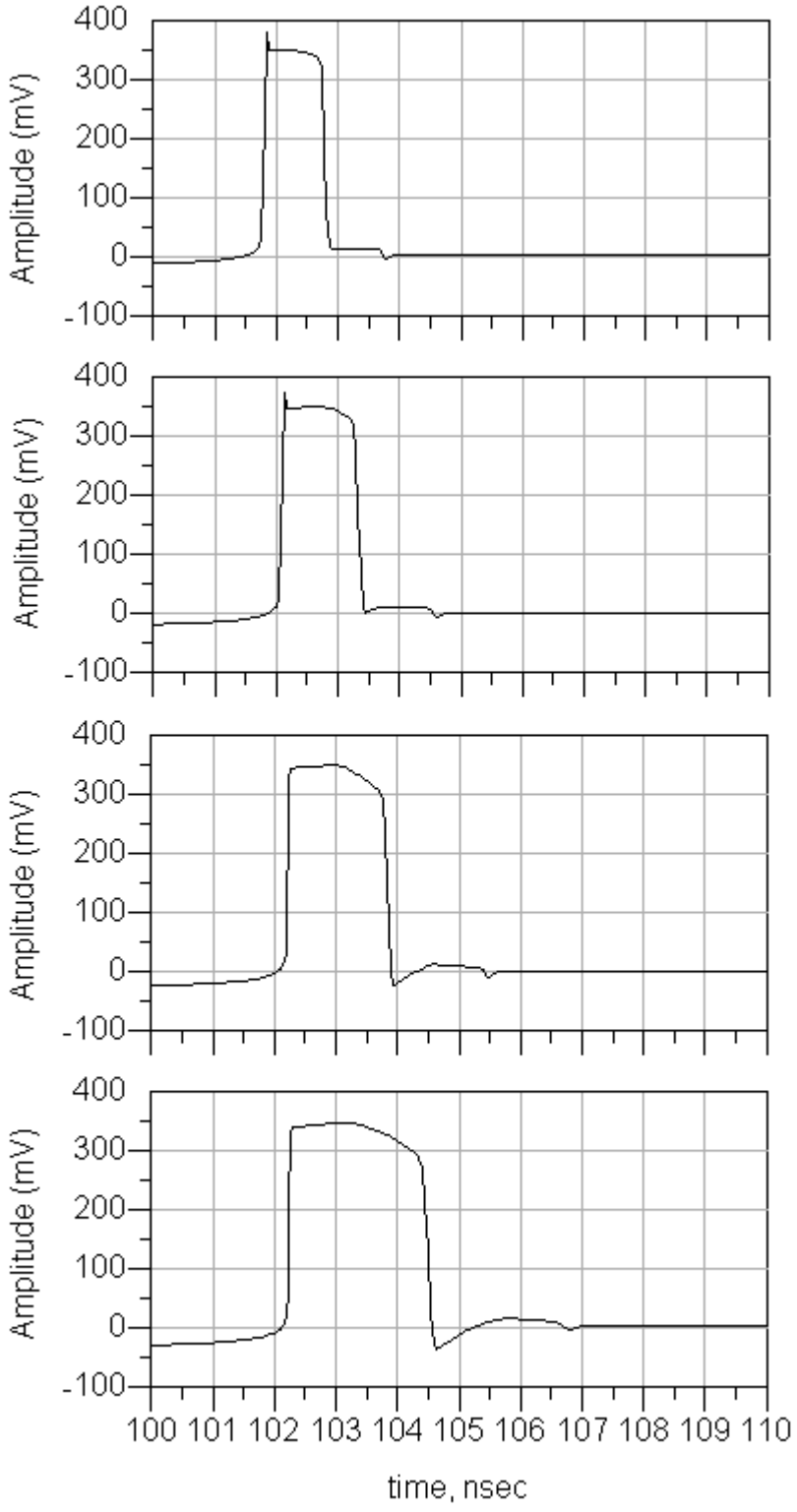

Figure 4.5.1 The ADS simulated pulses of 4-Bit digitally tunable UWB pulse generator

4.5.2 Measurement Results

The measured output pulse widths for 4-bit pulse generator range from 900 psec to 2400 psec with steps of 100 psec, which corresponds to bandwidth of 400 MHz to 1.1 GHz. In the **Figure 4.5.2**, the shortest, the longest and the other two time pulses among 16 output pulses are plotted on the same graph. Amplitude of the pulse output is around 300 mV when the applied input signal has a peak of 1.4 V at a frequency of 20 MHz. The output pulse of the generator can be easily used in and it can improve the performance of UWB GPR systems since most GPR systems are designed to work between 0.1 and 1.5 GHz [19, 20].

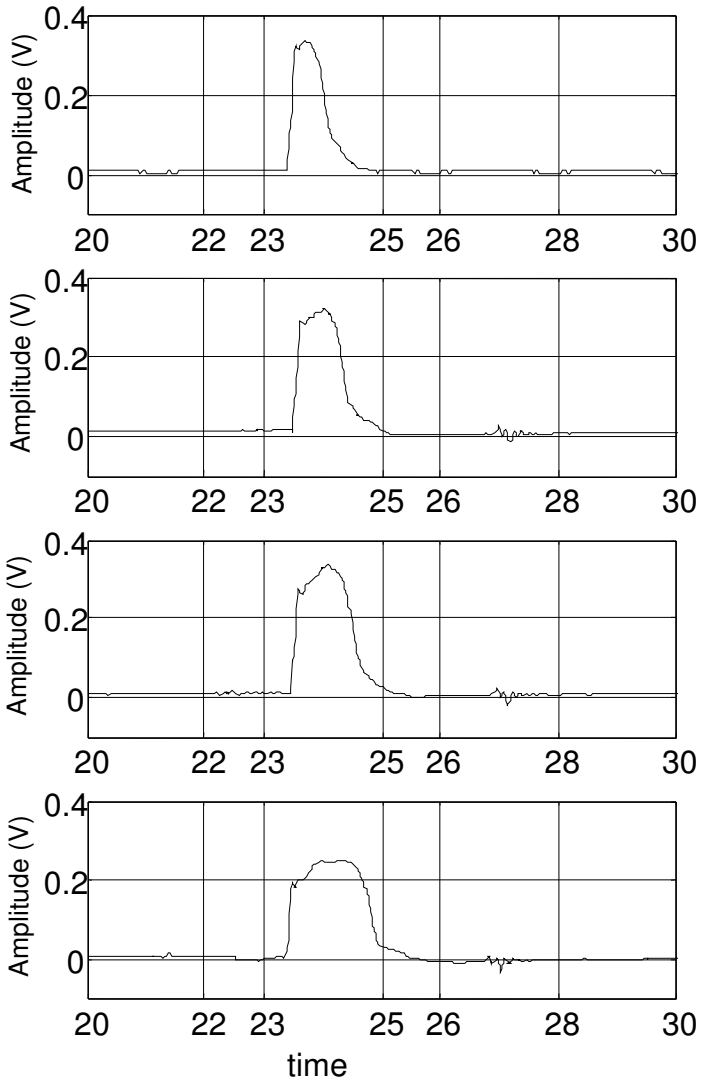

Figure 4.5.2 Measured output pulses generated by 4-Bit UWB pulse generator circuit

Also, one should note that the resolution of the pulse generator increases when the numbers of phase shifter sections are increased; however, this limits the frequency bandwidth since the group delays of the PIN diodes and dc blocking capacitors increase as more sections are placed into the circuitry. Therefore, there is a trade off between the frequency bandwidth and the resolution that can be obtained.

CONCLUSIONS AND FUTURE WORK

In this thesis, an UWB signal generator for an impulse type of pulse generator is described. 2-bit and 4-bit versions of N-bit digitally tunable UWB pulse generator using SRD, microstrip line delay lines and PIN diodes are presented. The working principle of the circuit; the applied input low frequency signal is initially converted to a step function by using SRD in order to create the sharp edges in the step function and latterly the sharp edges in step function are transformed into very short Gaussian like UWB pulses by using parallel short circuit stub. The parallel short circuit stubs include 2 and 4 PIN diodes/transmission line sub-sections, respectively. Each of the sub-sections is a high frequency diode switch; however, the sub-sections are re-designed for phase shifting. In every sub-section, a transmission line is connected to the PIN diode in parallel as a delay element and two PIN diodes are connected to the transmission line in series in order to avoid the reflections. The sub-sections are controlled digitally; in other words each sub-section is managed separately so that we could get 4 and 16 UWB pulses having different pulse durations from the 2-bit and 4-bit versions of N-bit digitally tunable UWB pulse generator, respectively. The simulated and measured pulse widths are in agreement and the pulse width changes from 550 psec (~2 GHz bandwidth) to 1750 psec (~550 MHz bandwidth) for 2-section version and changes from 900 psec (~1.1 GHz bandwidth) to 2400 psec (~450 MHz bandwidth) for 4-section version, which can be considered as an UWB pulse. The minimum pulse width is determined by the transition time of the employed SRD and the group delays of the PIN diodes and DC blocking capacitors changed with the number of phase shifter sections.

Also, the monocycle type pulses can be easily obtained by using the similar circuitry, which is used to obtain the UWB pulse. The circuit of the generator is low-cost and the generator can be easily used in many UWB applications like GPR, UWB radar and UWB positioning applications since the working frequencies of the generated

pulses are sufficient for the applications and the amplitude can be improved by using a bias circuit for the SRD.

As a future work, the generator circuit can be combined with differentiator circuits in order to get shorter pulses so that the flexibility of the generator can be improved. Also, the pulse generator circuit can be adapted to an UWB radar system in order to evaluate the performance of the pulse generator and observe the effect of the tunable pulse generation on the performance of the radar.

REFERENCES

[1] H.L. Bertoni, L. Carin and L.B. Felsen, editors, "Ultra-Wideband short pulse electromagnetic", 1992, New York, Kluwer Publications.

[2] C.L. Bennett and G.F. Ross, "Time-domain electromagnetic and its applications", Proceedings of IEEE, Vol. 66, No.3, pp. 29-318, 1978.

[3] Ultra Wideband Tutorial, "IEEE P802.15 Working group for WPAN document", doc. No. IEEE 802.15-00/083r0, March 2000.

[4] J. Foerster and et. Al, "Ultra-Wideband Technology for Short- or Medium Range Wireless Communications", Intel Technology Journal Q2, 2001.

[5] Byunghoo Jung, Yi-Hung Tseng, Jackson Harvey, and Ramesh Harjani, "Pulse Generator Design For UWB IR Communication Systems", IEEE Comm Letters, 2005.

[6] Arne Svensson, "Introduction to and Some Results on DS-UWB, Multiband UWB and Multiband OFDM", WIP/BEATS/CUBAN Workshop, Visby, August 2004.

[7] "Understanding UWB", IEEE P802.15 working group document, doc. No. IEEE 802.15-03/157r0, March 2003.

[8] J. S. Lee, Cam Nguyen, Scullion T., "A novel, compact, low-cost, impulse ground-penetrating radar for nondestructive evaluation of pavements", IEEE

Transactions on Instrumentation and Measurement, Volume: 53, Issue: 6, Dec. 2004.

[9] Aniruddha Rangnekar, Krishna M. Sivalingam. "Multiple Channel Scheduling in UWB based IEEE 802.15.3 Networks," broad nets, pp. 406-415, First International Conference on Broadband Networks (BROADNETS'04), 2004.

[10] Jeong Soo Lee; Cam Nguyen, "Novel low-cost ultra-wideband, ultra-short-pulse transmitter with MESFET impulse-shaping circuitry for reduced distortion and improved pulse repetition rate", IEEE Microwave and Wireless Components Letters, Volume 11, Issue 5, May 2001 Page(s): 208 – 210.

[11] J. Ha, C. Nguyen, "A new ultra-wideband, ultra-short monocycle pulse generator with reduced ringing", IEEE Microwave and Wireless Components Letters, Volume: 12, Issue: 6, June 2002.

[12] J. Han and C. Nguyen, "Ultra-Wideband Electronically Tunable Pulse Generators", IEEE Microwave And Wireless Components Letters, Vol. 14, No. 3, March 2004.

[13] Pochanin, G.P., "Problems and promising lines of development of UWB ground penetrating radiolocation", Ultra-wideband and Ultra short Impulse Signals, 2004 Second International Workshop 19-22 Sept. 2004 Page(s): 61 – 66.

[14] Stephen H. Kratzet, "Ultra Wide Band (UWB) Transmitter and Receiver Simulation using On/Off Keying (OOK)", Elanix Inc., Oct. 2002.

[15] Stephen H. Kratzet, "Ultra Wide Band (UWB) Transmitter and Receiver Simulation using Pulse Position Modulation (PPM) Either a Digital or Analog Data Source may be used", Elanix Inc., May 2003.

[16] M. J. Chudobiak, "New Approaches For Designing High Voltage, High Current Silicon Step Recovery Diodes for Pulse Sharpening Applications", PhD Thesis.

[17] R. Ludwig, P. Bretchko, “RF Circuit Design Theory and Applications”, New Jersey, Prentice Hall Inc., 2000.

[18] Sertac Yilmaz, I. Tekin, “Ultra-Wideband N-Bit Digitally Tunable Pulse Generator”, IEEE International Conference on Ultra-Wideband, Sept. 2005.

[19] U. Uschkerat, “Comparing UWB GPR measurements and simulation of simple shaped buried targets”, Detection of Abandoned Land Mines, 1998. Second International Conference on the (IEE Conf. Pub. No. 458) 12-14 Oct. 1998 Page(s): 41 – 44.

[20] Young-Jin Park, Sung-Bae Cho, Kwan-Ho Kim, Dong-Gi Youn, “Development of an ultra wideband ground penetrating radar (UWB GPR) for nondestructive testing of underground objects”, IEEE Antennas and Propagation Society Symposium, 2004, Volume 2, 20-25 June 2004 Page(s): 1279 - 1282 Vol.2.

APPENDIX

APPENDIX A

Novel Low-Cost Ultra-Wideband, Ultra-Short-Pulse Transmitter with MESFET Impulse-Shaping Circuitry for Reduced Distortion and Improved Pulse Repetition Rate

Jeong Soo Lee and Cam Nguyen

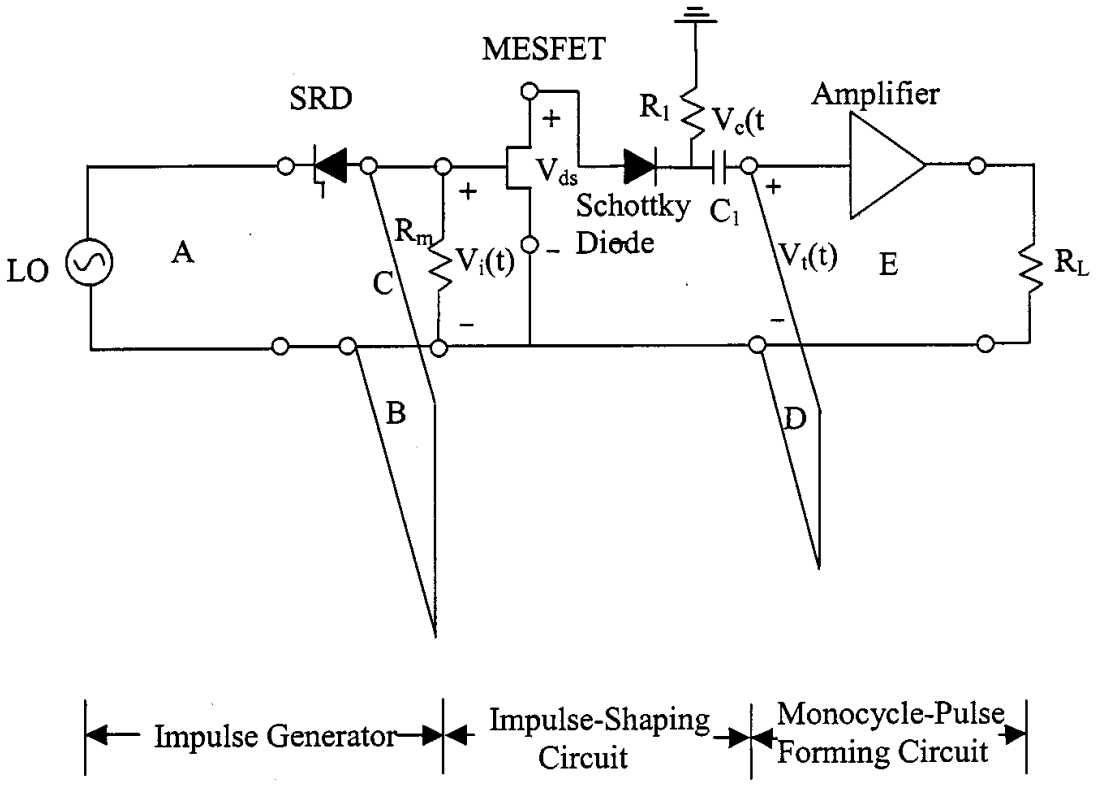

Figure A.1 Schematic of the new UWB, ultra-short-pulse transmitter. Bias circuits for the MESFET and amplifier are not shown.

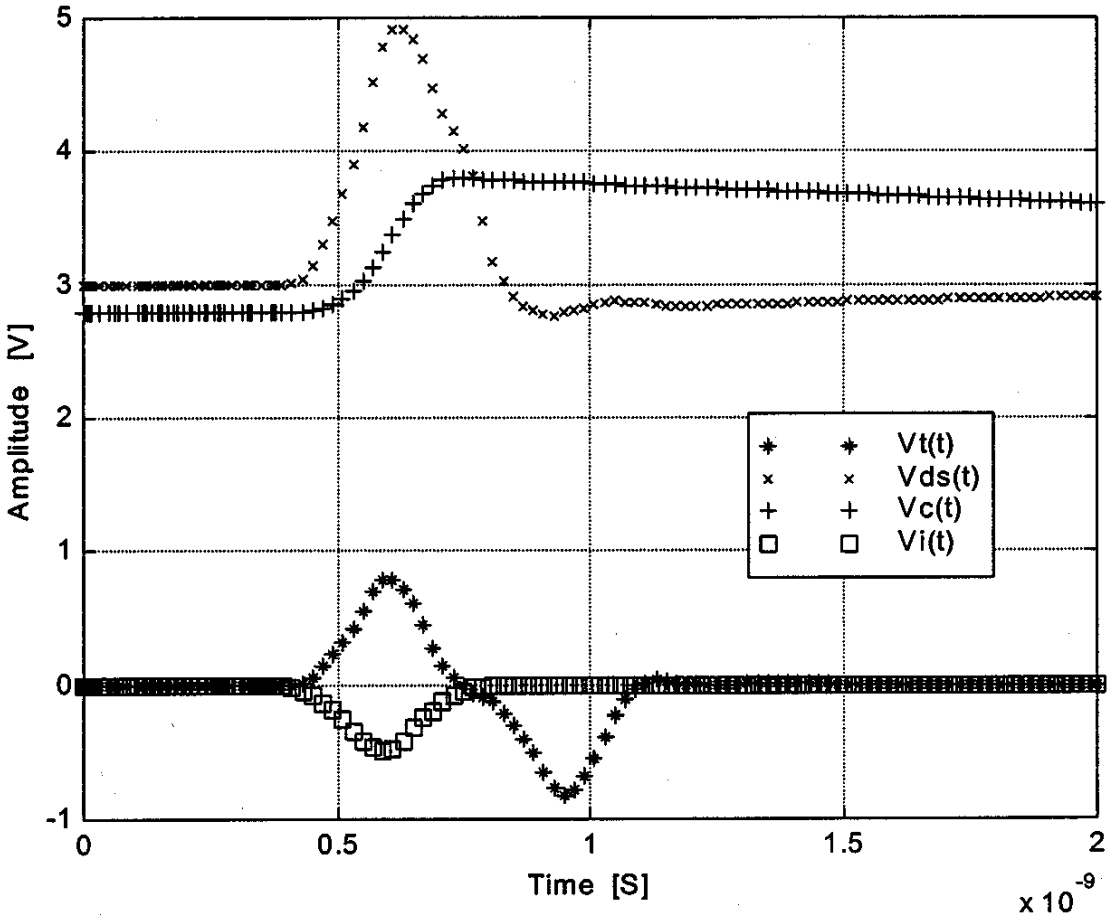

Figure A.2 Transient voltages indicated in Fig. 1.

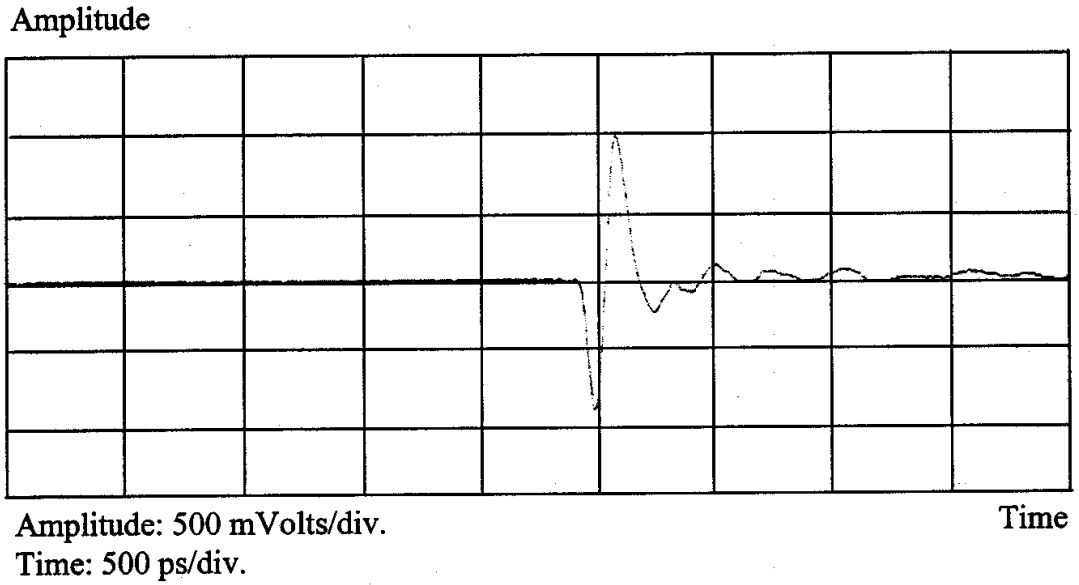

Figure A.3 Measured output pulse of the transmitter.

A New Ultra-Wideband, Ultra-Short Monocycle Pulse Generator With Reduced Ringing

Jeongwoo Han and Cam Nguyen

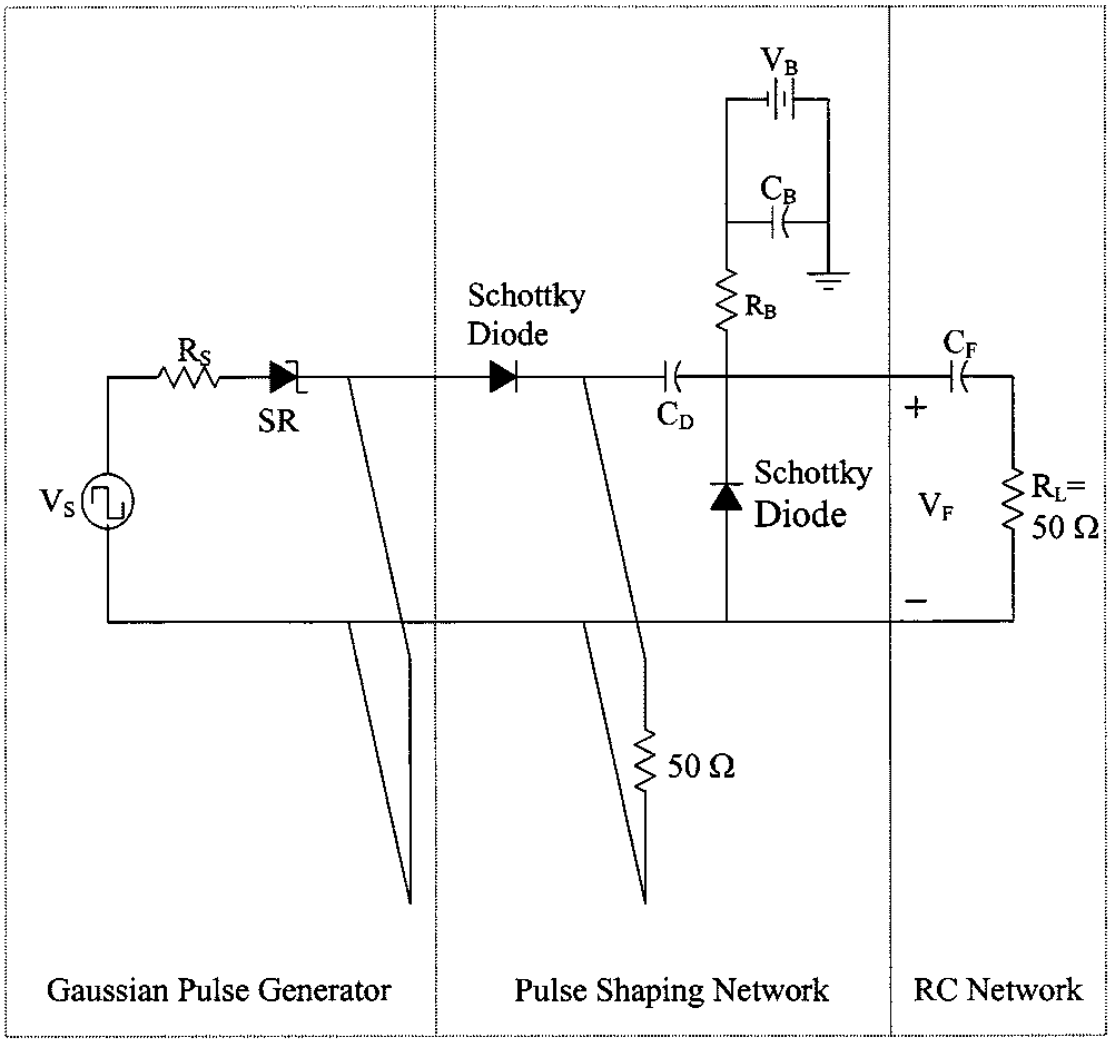

Figure A.4 Schematic of the new monocycle pulse generator.

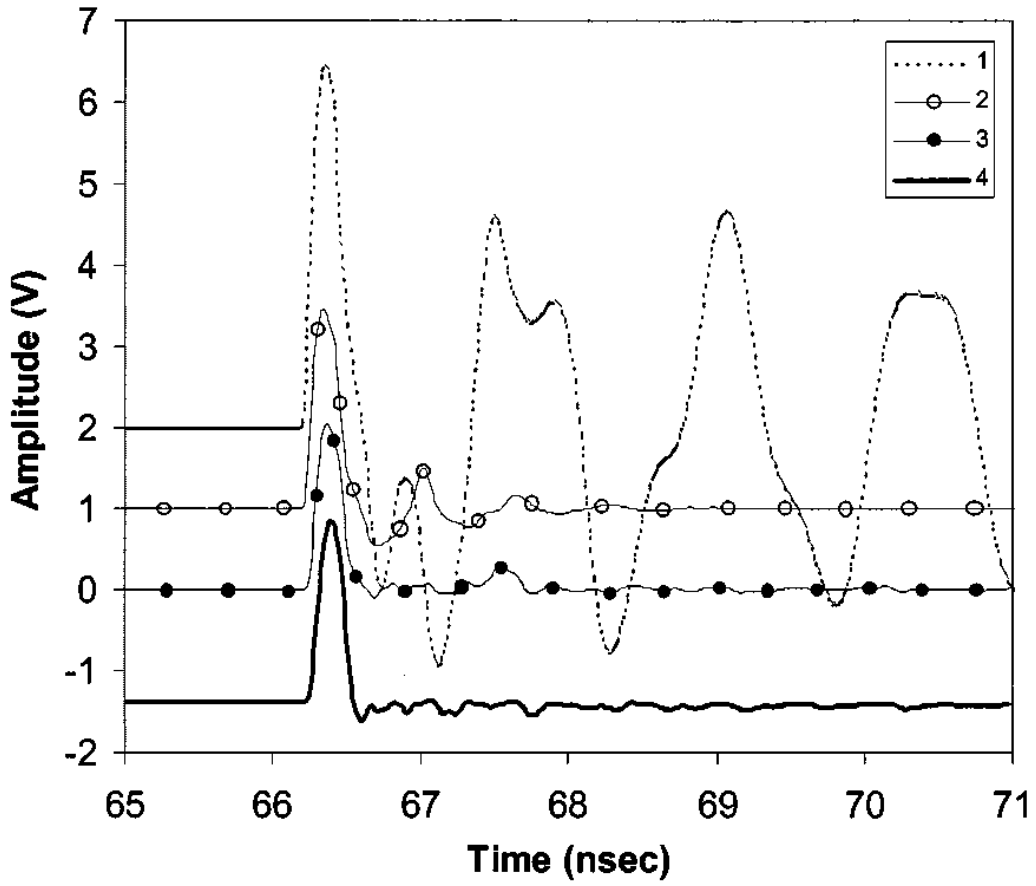

Figure A.5 Calculated voltage waveform at the input of the RC network (V in Fig.A.4). 1: Without pulse-shaping network; 2: with 50-ohm terminated shunt stub; 3: with 50-ohm terminated shunt stub and series Schottky diode; 4: with pulse-shaping network. Note: Waveforms 1, 2, and 4 are shifted by 1.5, 1, and _1 V, respectively, from their calculated results for easy distinction.

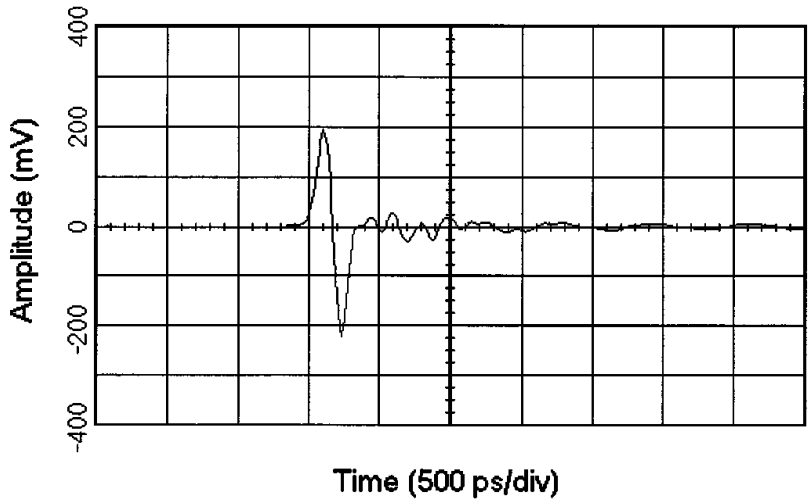

Figure A.6 Measured monocycle pulse.

APPENDIX B

Step Recovery Diode (MSD 700 Series)

Description

The **Micrometrics** MSD 700 series Step Recovery diodes are epitaxial silicon varactors which provide high output power and efficiencies in harmonic generator applications. Strict material and process controls result in high reproducibility. A unique silicon dioxide passivation process assures greater stability, reliability and low leakage currents at high temperatures. Diodes are available in various capacitance ranges for each of the 4 voltage ratings. These diodes represent the lowest transition times (snap time) available for each voltage rating. Unless otherwise specified, capacitance will be within the range shown above for each type. A capacitance tolerance of ±10% is available at an additional charge. Diodes can be optimized for custom electrical or mechanical specifications. Custom parameters for capacitance, voltage, transition time, series resistance, etc. are available upon request.

Applications

The MSD 700 series Step Recovery diodes are used as harmonic generators for all orders of multiplication, x 2 through x 20, for both narrow and wide bandwidths. Applications include local oscillators, voltage controlled oscillators, frequency synthesizers and up converters. They are also used in comb generators to generate a broad frequency spectrum and in high speed pulse shaping circuits.

Features

- Wide Selection of Tightened Capacitance Ranges
- Low Transition Times
- High Efficiencies

Packaging

- Chip, Glass, Ceramic, Surface Mount, Beam Lead

Junction Capacitance, Cj1 @ -6V, 1MHz (pF)	Minimum Breakdown Voltage, Vb @ 10 µA (V)	Minimum Carrier Lifetime,Tl Ir 6 mA, lf = 10 mA (nS)	Maximum Transition Time, Tt (pS)	Maximum Series Resistance, Rs 2 lf = 25 mA Rs (Ohms)	Maximum Thermal Resistance3 Θ Cj°C/W	Part Number
0.2 - 0.4	15	8	60	1.20	125	MSD700
0.4 - 0.6	15	8	60	1.00	100	MSD701
0.6 - 0.8	15	8	60	0.70	100	MSD702
0.8 - 1.0	15	8	60	0.50	75	MSD703
1.0 - 1.4	15	8	60	0.40	75	MSD704
1.4 - 2.0	15	8	60	0.30	60	MSD705
2.0 - 3.0	15	8	60	0.25	60	MSD706
0.2 - 0.4	20	11	70	1.00	100	MSD710
0.4 - 0.6	20	11	70	0.70	75	MSD711
0.6 - 0.8	20	11	70	0.60	75	MSD712
0.8 - 1.0	20	11	70	0.50	75	MSD713
1.0 - 1.4	20	11	70	0.40	75	MSD714
1.4 - 2.0	20	11	70	0.30	60	MSD715
2.0 - 3.0	20	11	70	0.25	60	MSD716
0.2 - 0.4	30	17	100	0.80	75	MSD720
0.4 - 0.6	30	17	100	0.60	60	MSD721
0.6 - 0.8	30	17	100	0.50	60	MSD722
0.8 - 1.0	30	17	100	0.40	60	MSD723
1.0 - 1.4	30	17	100	0.30	60	MSD724
1.4 - 2.0	30	17	100	0.25	50	MSD725
2.0 - 3.0	30	17	100	0.20	50	MSD726
0.2 - 0.4	40	21	150	0.80	50	MSD730
0.4 - 0.6	40	21	150	0.60	50	MSD731
0.6 - 0.8	40	21	150	0.50	50	MSD732
0.8 - 1.0	40	21	150	0.40	50	MSD733
1.0 - 1.4	40	21	150	0.30	50	MSD734
1.4 - 2.0	40	21	150	0.25	40	MSD735
2.0 - 3.0	40	21	150	0.20	40	MSD736

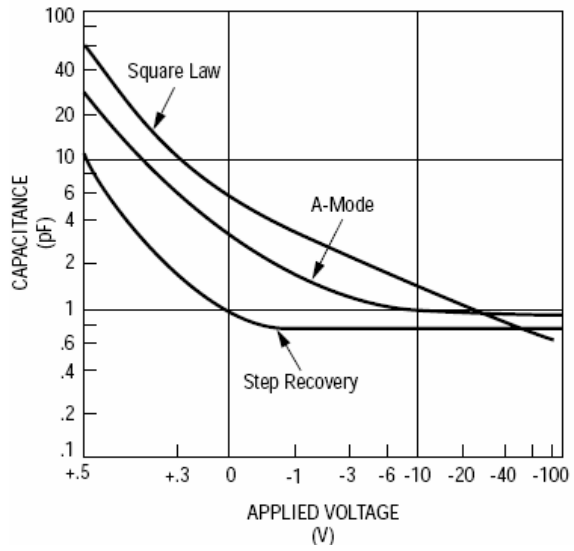

PIN Diodes (MMP 7000 Series)

Description

The **Micrometrics** MMP 7000 series PIN diodes are manufactured using very high resistivity silicon epitaxial material grown on a highly doped low resistivity substrate. Combined with a grown junction P++ layer, this yields a very abrupt structured "I" region with minimum outdoping and low voltage punchthrough characteristics. Our high temperature passivation and state of the art metallization produce diodes that are designed to cover a wide range of applications those fall into the general categories of switching, phase switching, attenuating and limiting. These devices are rugged and able to meet all visual criteria in space and military applications.

Applications

The MMP series are used in switch applications which include high speed low power switches, medium speed higher power switches, high power switches and attenuators, TR switches, digital phase shifters and duplexers.

Features

- High Temperature Passivation for Reliability
- Grown Junction for sharp "I" Region Interface
- Full Area Gold Contact for the Lowest Capacitance and Largest Bonding Pad Available
- Lot Traceability and Lot Control, Assuring High Reproducibility

Packaging

- Chip, Glass, Ceramic

Ultra Fast Switching							
Vbr1 MIN	**Cj-10 V2 MAX**	**Tl3 TYP**	**∅jc MAX**	**TS. Max.**	**RS@ 50 MA**	**RS@ 10 MA**	**Part Number**
(V)	**(pF)**	**(nS)**	**°C/W**	**NS**	**OHMS MAX**	**OHMS TYP**	
25	.1	10	60	1.5	.7	1	MMP7010
25	.15	10	50	1.5	.55	.8	MMP7011
25	.2	10	40	1.5	.45	.7	MMP7012
25	.25	10	35	1.5	.4	.6	MMP7013

Fast Switching, Low Power							
Vbr1 MIN	**Cj-10 V2 MAX**	**Tl3 TYP**	**∆jc MAX**	**TS. MAX.**	**RS@ 75 MA**	**RS@ 20 MA**	**Part Number**
(V)	**(pF)**	**(nS)**	**°C/W**	**NS**	**OHMS MAX**	**OHMS TYP**	
70	.05	60	80	5	.9	1.2	MMP7020
70	.1	60	70	5	.7	1.0	MMP7021
70	.15	60	60	5	.6	.9	MMP7022
70	.2	60	55	5	.5	.7	MMP7023
70	.25	60	50	5	.45	.5	MMP7024
100	.03	100	90	10	1.2	1.9	MMP7025
100	.07	100	80	10	.9	1.5	MMP7026
100	.1	100	70	10	.7	1.2	MMP7027
100	.15	100	60	10	.6	1.0	MMP7028
100	.2	100	55	10	.5	.9	MMP7029
100	.3	100	50	15	.45	.8	MMP7030
200	.03	225	90	15	1.9	3.0	MMP7031
200	.07	225	80	15	1.2	2.2	MMP7032
200	.1	225	70	15	.9	1.6	MMP7033
200	.15	225	60	15	.8	1.0	MMP7034
200	.2	225	55	15	.7	.8	MMP7035
200	.3	225	50	15	.6	.7	MMP7036

Operating Temperature	-55°C to 150°C
Storage Temperature	-65°C to 200°C
Reverse Breakdown Voltage (Vbr)	from 25 volts to 500 volts at 10 µA
Junction Capacitance (Cj-10)	from .03 pF to .5 pF at 10 volts
Switching Speed (TS)	from 1 nS to 25 nS
Lifetime (Tl)	from 5 nS to 2.0 µS
Chip Thickness	.004 - .007”thick

RF Choke (ADCH-80 Series)

	FREQUENCY (MHz)	INSERTION LOSS (dB)		VSWR (:1)		DC CURRENT (mA)	INDUCTANCE (µH) Typ.		
MODEL NO.		Typ.	Max.	Typ.	Max.	Max.	@ 0 mA	@ 50 mA	@ 100 mA
ADCH-80*	50 - 8000	0.3	1.0	1.1	1.35	100	7.0	1.8	1.0
	50-10000	0.3	2.0	1.1	1.6				
ADCH-80A*	50 - 8000	0.3	1.0	1.1	1.35	100	7.0	1.8	1.0
	50-10000	0.3	2.0	1.1	1.6				
TCCH-80	50-8200	0.5	1.1	1.1	1.7	100	4.0	1.3	0.9

Features;

- low parasitic capacitance 0.1 PF typ.
- 50 Ω
- Surface Mount
- effective parallel resistance, Rch 800 ohm typ. TCCH-80, Rch 500 ohm typ.
- TCCH, patent pending, miniature .15"X.15"

Applications;

- biasing amplifier
- biasing of laser diodes
- biasing of active antennas

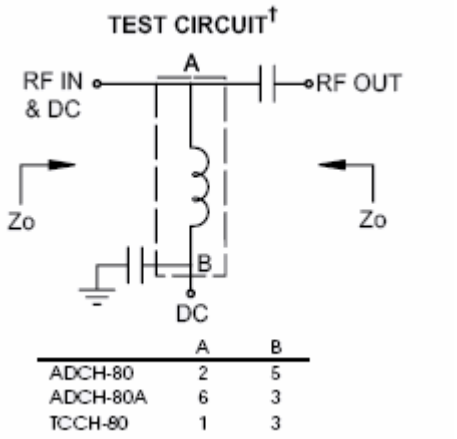

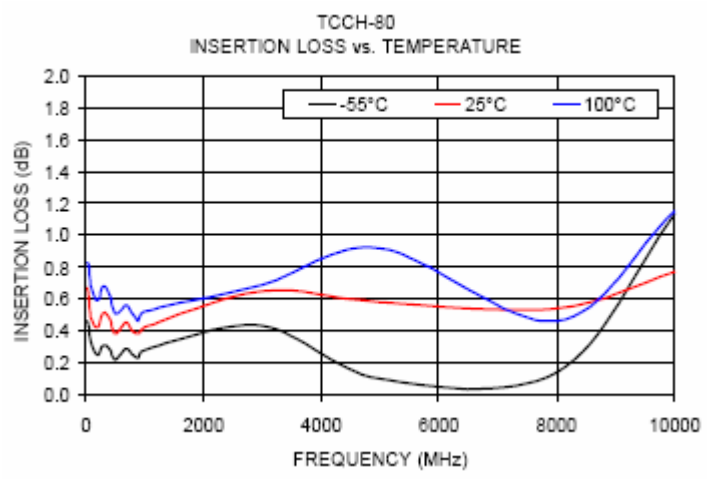
TCCH-80
INSERTION LOSS vs. TEMPERATURE
INSERTION LOSS (dB)
2.0
1.8
1.6
1.4
1.2
1.0
0.8
0.6
0.4
0.2
0.0
-55°C
25°C
100°C
0
2000
4000
6000
8000
10000
FREQUENCY (MHz)

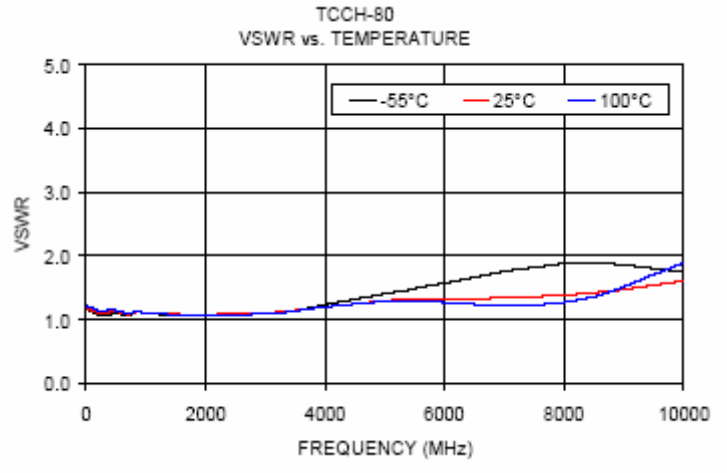
TCCH-80
VSWR vs. TEMPERATURE
VSWR
5.0
4.0
3.0
2.0
1.0
0.0
-55°C
25°C
100°C
0
2000
4000
6000
8000
10000
FREQUENCY (MHz)